

Electroluminescence of Charge-Transfer Fluorescent Donor-bridge-Acceptor Systems

J. W. Verhoeven, M. Goes and J. W. Hofstraat,
Laboratory of Organic Chemistry, University of Amsterdam,
and K. Brunner, Philips Research

Introduction

Over the last decennia a plethora of D-b-A systems has been investigated,¹⁻³ in which a rigid bridge unit (b) keeps electron donor (D) and electron acceptor (A) moieties separated at a distance way beyond the sum of their Van der Waals radii. Notwithstanding this spatial separation, photoexcitation of such D-b-A systems often has been found to induce the occurrence of rapid intramolecular electron transfer from D to A leading to an excited state with strong charge transfer (CT) character. It has been established beyond doubt, that the electronic interaction between D and A required to allow for such intramolecular electron transfer is in general mainly mediated via the bridge even if the latter consists of saturated hydrocarbon elements, which classically speaking prohibits conjugative transmission. Following the original proposal and description by Hoffmann et al.⁴ it is now generally accepted to indicate electronic interaction via a saturated framework as through-bond interaction (TBI), although regrettably some authors recently appear to be tempted to use this terminology also for transmission of electronic effects via conjugated bridges, which we feel to be a confusing generalisation ($B \neq b$!).

It is important to stipulate that, although in the weak coupling limit the rate of electron transfer scales with the square of the electronic interaction between D and A, a quite small electronic interaction (V_{DA}) already suffices to enable very fast electron transfer, if other factors are optimised. Thus under "optimal conditions"—which in general implies that a strong D/A pair is incorporated so that the driving force for electron transfer is large enough to compensate the overall reorganisation energy—typically a V_{DA} in the order of a few wavenumbers suffices to allow for electron transfer on a subnanosecond timescale. This is one of the reasons that the in general rather weak TBI typical for D-b-A systems with a saturated bridge structure is still strong enough to allow for the occurrence of intramolecular electron transfer in such systems. At the same time the weakness of TBI also implies that the oscillator strength of the direct electronic transition between the ground state and the CT state in such D-b-A systems is in general too small to make such a transition spectroscopically detectable. This is especially so with regard to the absorption spectra, which tend to be so similar to a superposition of the absorption spectra of the separate D and A chromophores that many authors are led to the conclusion that "there is no interaction in the ground state", whereas the conclusion should in fact be that the direct CT absorption is too weak to be detected under the overlapping strong local absorption bands of D and A.

Because of the characteristic large Stokes shift of CT fluorescence and the quenching of local D and A fluorescence upon photoinduced electron transfer it is more often possible to detect the radiative component of the charge recombination from the CT excited state to the ground state of D-b-A systems by emission spectroscopy. This type of emission is sometimes referred as intramolecular exciplex fluorescence, but we feel that for relatively rigid systems the term intramolecular CT fluorescence is more appropriate since "exciplex" should be reserved for situations where the interaction is established in the excited state by significant reorganisation, for example, reduction of D-A distance.

Continued on page 3

From the Executive Director

D. C. Neckers, Executive Director, Center for Photochemical Sciences, Bowling Green State University

This year marks the fifteenth anniversary of *The Spectrum*. What started as an unknown four-page newsletter distributed to 400 scientists is now a well-respected publication with over 7,000 people in 70 countries receiving it via the web or mail.

My original idea for *The Spectrum* was to relate interesting happenings in the photochemical sciences in a more informal and timely fashion than a refereed journal. *The Spectrum* is targeted primarily to an audience of photoscientists, but is general enough to appeal to others. Non-photoscientists also read it to keep abreast of technical discoveries in fields outside their own.

The Spectrum is now abstracted by *Chemical Abstracts* and, more recently, by the *Abstracts Journal* of the All-Russian Institute of Scientific and Technical Information of the Russian Academy of Sciences. After the fall of the Soviet regime in the late 1980s, *The Spectrum* assumed a primary literature role in many countries. It was for many one of the only sources of original scientific information. One of our secrets—distribution of *The Spectrum* without charge—was particularly important in this respect. It was a struggle for us on occasion, but we have never backed away from that original modus operandi. The idea was and still is to provide a service to the photochemical and scientific community as part of the outreach mission of the Center for Photochemical Sciences.

The Spectrum has always provided a unique vehicle to relate news to the scientific community at large about the Center for Photochemical Sciences, a focused research entity in a small university in Ohio that was trying to assume a more important role in higher education. At the time *The Spectrum* was begun, we had no Ph.D. program at Bowling Green. Now we admit about 16-18 new Ph.D. students a year and graduate, on average, 8-10 new Ph.D.s each year. As our program has evolved, we have watched our graduates assume new and different roles in large, multi-national companies, while others have joined companies funded by venture capital and the dream of one or more creative entrepreneurs. In an issue later this year we will publish in *The Spectrum* an article written by one of our first graduates, Dr. Lisa Kelly, recently promoted to associate professor at the University of Maryland, Baltimore County, Department of Chemistry and Biochemistry. Lisa will contribute the very first article written by one of our Ph.D. graduates.

A year or so ago one of our graduate students, as part of a required course in literature studies in the photosciences, offered a report on a new technique for the class. At the very end she let the class in on her secret. She had gotten the information for her article from a recently submitted article to *The Spectrum*. The class had not seen it yet since it had not been published.

This anniversary provides us with an impetus to expand and improve. *The Spectrum* is exploring new ways to increase our coverage of the photosciences and the research, people, and events that keep it at the technological forefront of science. As the changes take root, *The Spectrum* will become a stronger publication that better serves the interests of the photochemical community and related fields of endeavor. As always I welcome any feedback and ideas for new directions. We look forward to sharing our new ideas in upcoming issues.

In This Issue

Electroluminescence of Charge-Transfer Fluorescent Donor-bridge-Acceptor Systems	1
From the Executive Director	2
Technical Note: SLM 48000 Spectrofluorimeter Non-Volatile Memory IC Replacement	13
Cross-quenching Investigations of Platinum(II) Diimine Complexes	14
Science and Technology of Organic Light Emitting Diodes	20

Continued from page 1

Although detectable in various conformationally extended D-b-A systems, such CT fluorescence tends to be weak since the radiative rate constant (k_r) also scales with the square of V_{DA} and is thus typically small,⁵ which implies that even moderately fast non-radiative decay processes (k_{nr}) reduce the fluorescence quantum yield (Φ): $\Phi = k_r / (k_r + k_{nr})$.

Charge Transfer Fluorescence of D-b-A Systems of the FP and FT Type

During our extensive research on through-bond coupled D-b-A systems we have encountered some remarkable exceptions to the rule of weak CT absorption and fluorescence for D-b-A systems with a rigid, extended conformation. This refers in particular to a number of systems with a relatively short through-bond coupling pathway. Especially for several D-b-A systems with three sigma bonds separating D and A, but also in a few cases with up to five sigma bond separation, we detected discrete and relatively strong intramolecular CT absorption.^{2,6}

One of the earliest and most extensively studied examples is the aza-adamantane based system **NDCV** (see Figure 1).^{7,8} Here the tertiary amino nitrogen serves as the donor and the 1,1-dicyanovinyl as the acceptor separated from it by a minimum distance of three sigma bonds. Nevertheless **NDCV** displays an intramolecular CT absorption with a maximum around 320 nm and a molar extinction as high as $\epsilon = 4500 \text{ M}^{-1} \cdot \text{cm}^{-1}$. While **NDCV** also displays clear CT fluorescence, its quantum yield is not spectacular because of competing dark processes.

The latter situation is dramatically different in compounds which we have dubbed fluoroprobes and fluorotropes. These are also characterised by a three bond D-A separation and a nitrogen based donor but the bridges involved are respectively of the piperidine and the tropane type while the acceptors are vinylaromatics.

The basic structures called Fluoroprobe (FP) **1**⁹ and Fluorotrope (FT) **2**¹⁰ are depicted in Figure 1.

The fluorescent properties of FP (**1**) and FT (**2**) as well as of various analogues—such as the FT analogues **3**, **4**, and **5**—that contain substituents at the para-position of the aniline-donor and/or in which the aromatic part of the acceptor is varied, have been studied extensively. The most remarkable feature of most of these systems is that they display exclusive CT fluorescence with a fluorescence quantum yield that (also depending on the medium) in some cases can be as high 80%. This strong CT fluorescence allows observation in many media, that is, in the gas phase,¹¹ in a wide variety of solvents,¹² on surfaces¹³ as well as in solid (polymeric) matrices.¹⁴⁻¹⁷ From such studies it has become evident that the enormous increase of the dipole moment of FT and FP like systems in the CT excited state makes the position of their CT fluorescence uniquely sensitive to the degree to which their molecular environment can respond to this giant dipolar state within its lifetime, which is typically in the nanosecond domain.

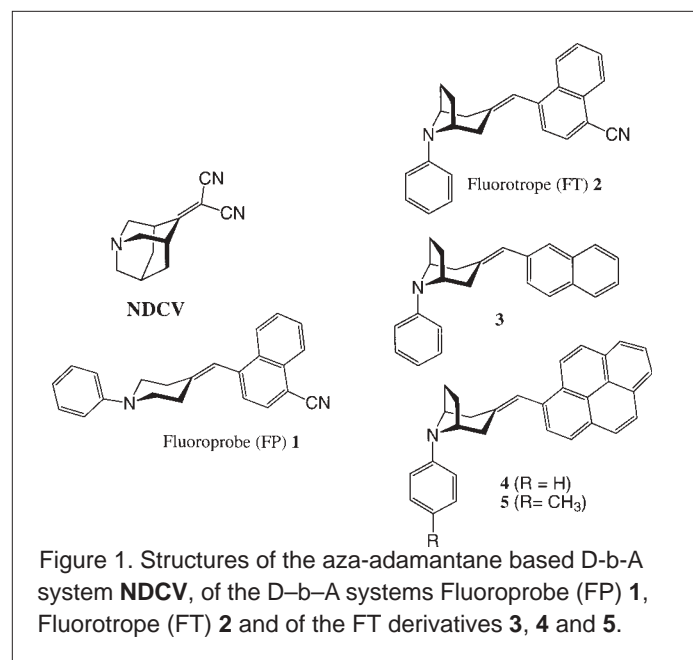


Figure 1. Structures of the aza-adamantane based D-b-A system **NDCV**, of the D-b-A systems Fluoroprobe (FP) **1**, Fluorotrope (FT) **2** and of the FT derivatives **3**, **4** and **5**.

Table 1 compiles typical CT fluorescence data for **1**–**5** in three solvents at room temperature. These data testify not only the enormous solvatochromism upon transfer from an essentially non polar solvent like cyclohexane to dipolar solvents but also the high quantum yields of CT fluorescence obtainable with this type of D-b-A systems. As expected the wavelength of the CT fluorescence maximum in each solvent shifts in response to changes in the donor and acceptor strength in the order $3 < 4 < 5 < 1 < 2$.

At room temperature dipolar reorganisation of solvent molecules typically occurs within picoseconds and therefore the CT fluorescence of FT and FP in liquid solution almost exclusively occurs after complete solvent reorganisation, which leads to an extreme solvatochromism expressed by a huge red shift with increasing solvent polarity (see Table 1). The situation can be very different when the molecular mobility of the surrounding medium is impeded, such as is the case when FT and FP are incorporated in solid matrices like high molecular weight polymers or in highly viscous

Table 1. CT fluorescence maxima, λ_{\max} , and quantum yields, Φ , for 1 - 5 in respectively cyclohexane/, di-n-butylether/, and tetrahydrofuran at room temperature.

	1	2	3	4	5
λ_{\max} (nm)	410 / 465 / 571	422 / 476 / 578	368 / 388 / 446	391 / 420 / 513	395 / 444 / 541
Φ (%)	21 / 85 / 16	61 / 74 / 25	12 / 29 / 37	56 / 84 / 67	69 / 70 / 60

and glassy media obtained by cooling of low molecular weight solvents. The latter allows FP and FT like systems to display extremely strong fluorescence thermochromism. A dramatic example¹⁸ is given in Figure 2 for the behaviour of FP in 2-methyltetrahydrofuran (MTHF). In this solvent FP displays yellow-greenish CT fluorescence similar to that in tetrahydrofuran (see Table 1) at room temperature. Cooling initially induces a red shift because at lower temperature the dielectric constant of the solvent increases while its dipolar reorganisation is still subnanosecond. However, upon cooling down into the supercooled liquid region (i.e. below the melting point of $T_{\text{mp}} = 135$ K) the solvent relaxation time increases to nanoseconds and rapidly increases further to seconds upon cooling to the glass transition point ($T_g = 91$ K). As a result more and more CT excited FP molecules emit before (complete) solvent relaxation thus leading to a dramatic blue shift of the emission maximum observed by continuous emission spectroscopy (see Figure 2) and remarkable dynamic Stokes shift phenomena in time resolved measurements.¹⁸

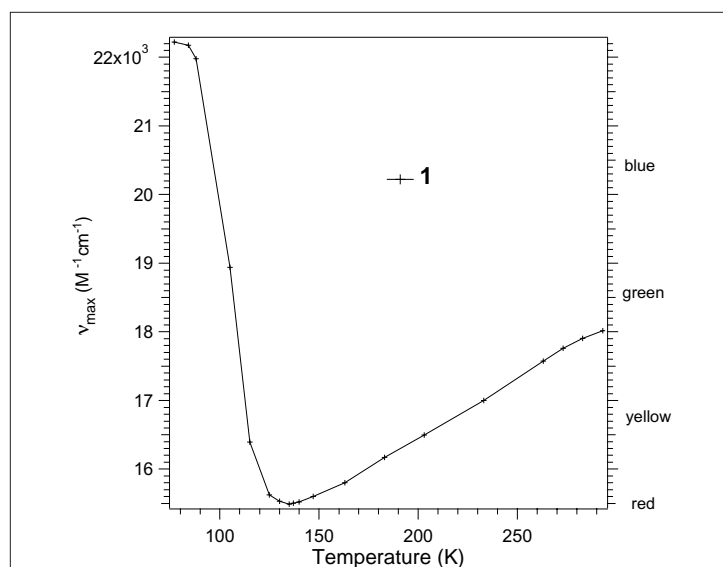


Figure 2. Thermochromic shift of the CT fluorescence maximum of FP (1) in 2-methyltetrahydrofuran.

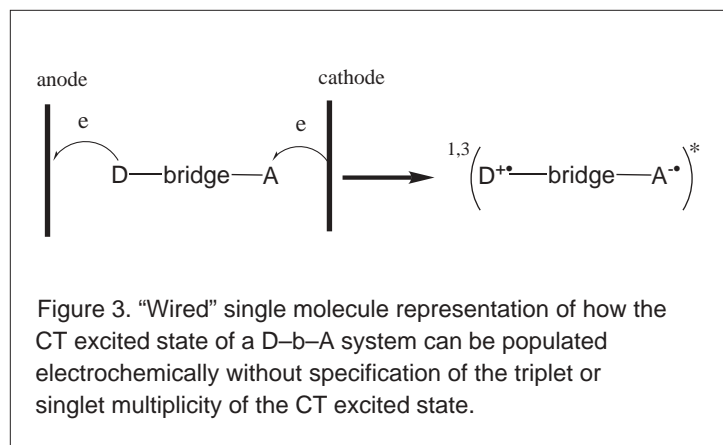


Figure 3. "Wired" single molecule representation of how the CT excited state of a D-b-A system can be populated electrochemically without specification of the triplet or singlet multiplicity of the CT excited state.

Electroluminescence

Mechanistic aspects of electroluminescence from D-b-A systems

It is evident that the CT excited state of D-b-A molecules cannot only be populated by photoexcitation but in principle also electrochemically. In a "wired" single molecule representation (see Figure 3), electrochemical one electron reduction of A and one electron oxidation of D provides a direct pathway to the CT excited state (not specifying the overall triplet or singlet spin state!).

As explained in the preceding section, D-b-A systems of the FP and FT type retain their strong CT fluorescent properties in solid matrices and because of the lack of rapid medium reorganisation this fluorescence in general occurs in a wavelength region corresponding to that where these D-b-A systems emit in low polarity solvents. For FP and FT, as well as for several of their analogues which we have studied, this implies that they emit blue CT fluorescence when incorporated in a solid matrix. When for an FP or FT analogue incorporated in a solid matrix the CT excited state could be generated electrochemically, this would thus provide an entry to a blue emitting electroluminescent device (i.e., a blue light emitting diode, LED). In such a device the anode and cathode will of course not be in direct contact with a single D-b-A molecule like suggested in Figure 3. However, when a thin film containing D-b-A molecules is sandwiched between two electrodes, one may envisage the mechanism outlined in eqs [1] – [4] and schematically visualised in Figure 4.

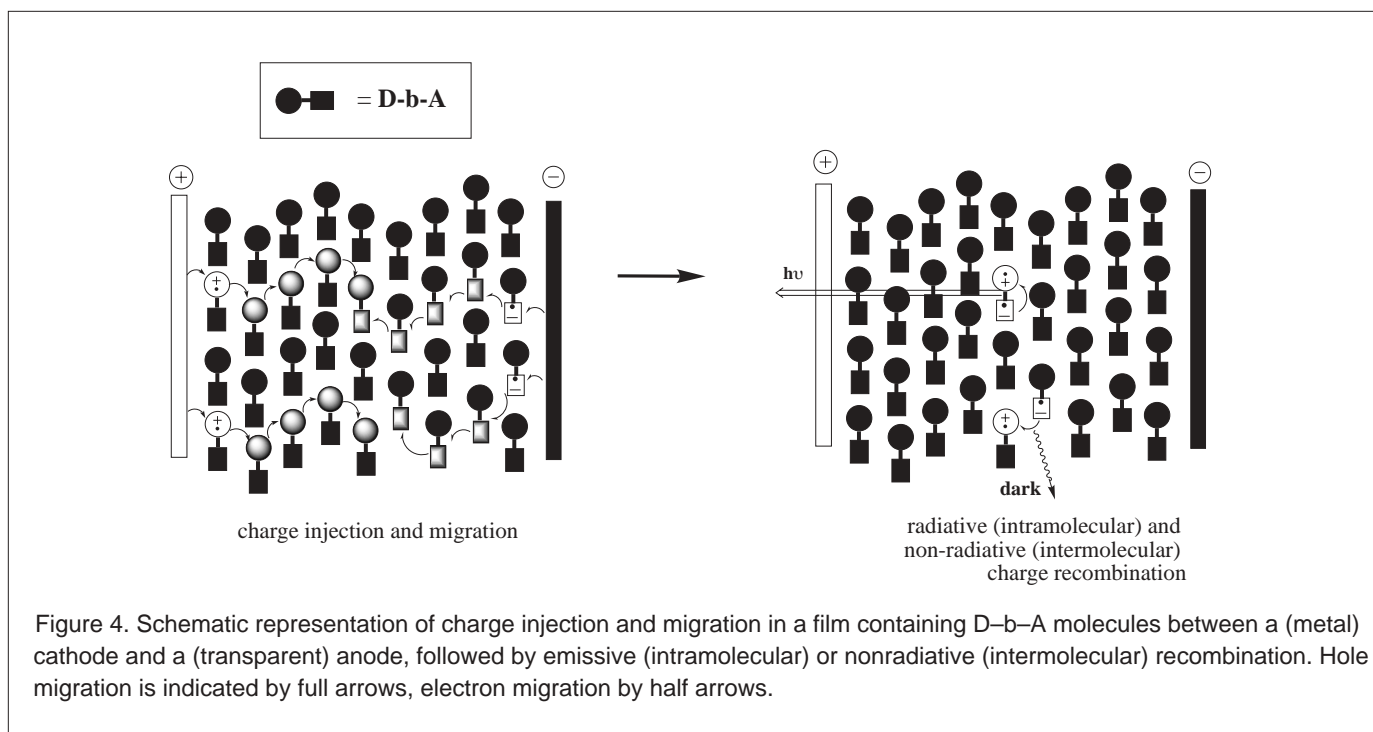


Figure 4. Schematic representation of charge injection and migration in a film containing D–b–A molecules between a (metal) cathode and a (transparent) anode, followed by emissive (intramolecular) or nonradiative (intermolecular) recombination. Hole migration is indicated by full arrows, electron migration by half arrows.



Steps [1] and [2] describe hole injection and electron injection in D-b-A molecules located respectively close to the anode and to the cathode. How close will depend on the conductive properties of the surrounding matrix (see later). Degenerate charge hopping between neighbouring D-b-A molecules is then required until a “hole” and “electron” reside on the same molecule (step [3A]), which is equivalent to formation of the CT excited state, that finally relaxes by intramolecular charge recombination under the emission of CT fluorescence, $h\nu_{\text{CT}}$, (step [4]).

Clearly the formation of the CT excited state in step [3A] is most crucial since it has to compete with the “dark” intermolecular charge recombination [3B]. It should be noted that the electron transfer process [3B] is much more exergonic than [3A], the difference being the energy of the CT excited state, which is in the order of 2.7 - 2.1 eV as judged by the energy of the CT emission maximum. This implies that [3B] occurs far in the Marcus¹⁹ inverted region, which may slow it down sufficiently to make [3A] the favoured mode of electron exchange when “hole” and “electron” meet. In eq [3B] as well as in Figure 4 it has been tacitly assumed that intermolecular charge recombination—in contrast to intramolecular charge recombination—has no radiative component. This is because, while FP and FT like systems are known to display very strong photoinduced, intramolecular CT fluorescence in dilute solution (see Table 1) as well as when doped in polymer matrices, it has been found that mixing of model D and model A systems does not produce detectable intermolecular (exciplex type) CT fluorescence but only leads to quenching of the local D and A fluorescence.

It seems important to point out that Figure 4 suggests that electroluminescence could in principle be induced from a layer of a pure D-b-A system. This is indeed the case as discussed elsewhere,²⁰ but it requires vapor phase deposition of the D-b-A system. Our prime interest, however, was to produce LEDs that can be deposited from solution by, for example, spincoating or inkjet printing. We will in this paper therefore concentrate upon LEDs where the D-b-A system is codissolved with a polymer in an organic solvent, which upon spin coating on a transparent anode (ITO on glass) yields a thin polymer layer doped with the D-b-A system. On top of this a low work function metal cathode is deposited.

In a preliminary communication²¹ it was reported that electroluminescence can indeed be realised when FP is doped into a thin polymer film between two electrodes. Here we report more extensively on the properties of composite polymer light-emitting diodes (PLEDs) based on this principle and containing more suitable FT derivatives.

Experimental Details

Materials for the diodes

The synthesis of the D-b-A compounds used (see Figure 1) has been described elsewhere.^{9,10,20,22} Poly(9-vinylcarbazole), PVK, (secondary grade Mw=69000) and polystyrene, PS, (Mw=280000) were obtained from Aldrich. Glass substrata of 30x30 mm² containing a conducting transparent indiumtin oxide, ITO, layer were obtained from Balzers and patterned at Philips Research.

Spincoating of thin films

Solutions were made of approximately 15 mg/ml polymer in solvents like tetrahydrofuran, toluene and dioxane. The luminescent probe is also added to the solution in concentrations of 1-20% (weight/weight of the polymer). From spincurves it was determined that 70 nm films could be obtained when using a 15 mg/ml solution that is spinned at 1500 rpm for 10 s followed by 30 s spinning at 500 rpm for drying. The optimal film thickness for our diodes is around 70 nm but in some cases a thickness around 100 nm was also employed to reduce the risk of short circuits.

Fabrication of diodes

The complete fabrication of LEDs was done under clean room conditions, starting with the cleaning of ITO patterned substrata (successive rinsing in soap, demiwater and isopropanol in a sonic bath). Prior to utilisation the ITO was irradiated with UV in an ozone atmosphere. The substrata and solutions or compounds were transferred to a nitrogen purged glovebox (MB150B-G, MBraun). The composite LEDs were constructed by spincoating from filtered polymer solutions using a programmable spincoater (Delta 20, BLE). The spincoated substrata were transferred to another compartment of the glovebox where metals could be evaporated to complete the devices. The deposition of the metal electrodes consisting of a thin layer of Ba coated (for protection) with a thicker layer of Al occurred through a mask, creating four square overlaps with the ITO anode, 0.075, 0.133, 0.316, 0.95 cm² in size. Evaporation occurred in a vacuum chamber controlled by a gauge (series 307, Granville-Phillips) with Pyrani element at pressures below 2x10⁻⁶ torr. The concentration of the elements in the atmosphere of the chamber under high vacuum was monitored using a massspectrometer (Quadstar 422, Balzers). The chamber contained two sources for metal evaporation. The layer thickness (and rate of evaporation) was monitored via the change in resonance frequency of a quartz crystal positioned next to the samples (Inficon XTC, Leybold Hereaus), and could be varied. For aluminium the best results were obtained with a rate of 0.5 nm/s (at 1 nm/s a lot of devices exhibited short-circuiting). For barium the rate was set at 0.3 nm/s.

Device characterisation

The LEDs were characterized by attaching a computer controlled low noise single channel DC power source that can act both as a voltage source or current source and a voltage meter or current meter (Keithley 2400, Keithley Instruments). In a typical characterisation of a LED the voltage is increased step wise from zero to a preset positive voltage (mostly 20 V but higher voltages are needed when the turn-on voltage is high), back to low voltage and ultimately to negative voltage. Light from the diode in forward direction is coupled into a photodiode and read out by an electrometer/high resistance meter (Keithley 6517, Keithley Instruments). The output of both meters is redirected to the computer. The control and the collection of the data is handled by a Labview (National Instruments) based program. Calibration of the photodiode is done at a fixed current with a luminance meter (LS-110, Minolta). For every diode with a different spectral distribution of light, the photocurrent as measured by the photodiode has to be correlated to the light output in cd/m².

A property of diodes that is used to characterize a device is the turn-on voltage. By definition this is the voltage at which a measurable current (above noise) starts running through the diode (turn-on voltage for current). If it were to be a perfect LED at this point it would also start emitting light (turn-on voltage for light), but this is not necessarily the case. Single carrier current can already flow through the device in absence of injection of charge carriers on the opposite side: the LED remains devoid of light. In the set-up we used, light can be detected above a level of ca. 0.05 cd/m². For recording the electroluminescence spectra outside the glovebox, a fibre coupled spectrograph (Spectra 150, Acton) connected to a Peltier cooled CCD camera (TEA/CCD-1024-EM1, Princeton Instruments) was used. When recording

an EL spectrum inside the glovebox another (less sophisticated) fibre coupled spectrograph/CCD camera combination (S2000, Ocean Optics) was used. The emission was afterwards corrected for the wavelength dependence of the spectrometer.

D-b-A Doped Polystyrene Diodes

In order to test the feasibility of PLEDs with a D-b-A system as the only electroactive component, we produced via the methods described in the experimental section several diodes in which the organic layer consists of the highly insulating polymer polystyrene (PS) doped with various amounts of a D-b-A compound.

Spincoating of a 20 mg/ml co-solution of polystyrene (PS) and a D-b-A compound in toluene at 2000 rpm yielded 110 nm films. All diodes were covered with a barium electrode (and aluminium on top of the barium). Under forward bias the devices produce blue light! Figure 5 shows that the prepared devices behave more or less like a diode and that the observed blue light can be measured. Notice that under reversed voltage there is little current and no light at all.

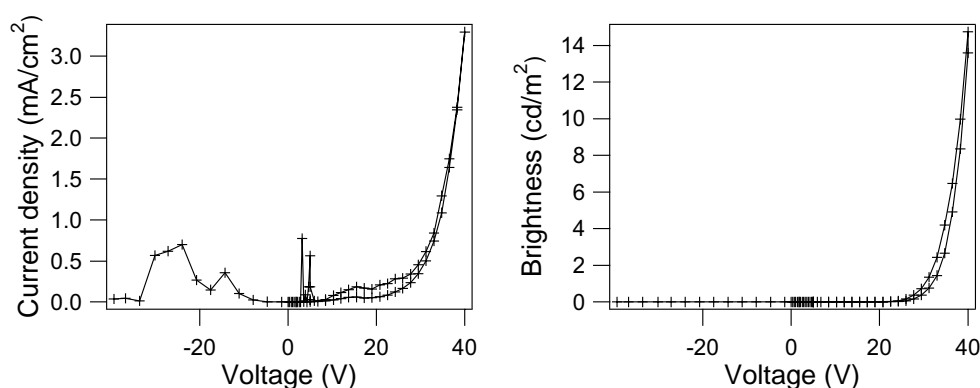


Figure 5. Current density (left) and brightness (right) vs. the voltage over a polystyrene diode comprising 10% of **2**; under negative bias no light and little current is observed.

As can be seen from Figure 6 the concentration of the D-b-A compound is crucial for the performance of the diode. Upon increasing the concentration from 5% to 10% of **2** the turn-on voltage for light shifts from *circa* 25 V to 22 V. This might be a result of the fact that the light of the diode containing 10% of **2** is detected in an earlier stage (the photodiode is more sensitive towards red-shifted electroluminescence). It appears as if the turn-on for current is at about the same voltage. More light is produced at lower voltages upon increasing concentration of **2**, and also the maximum efficiency goes up from 0.25 cd/A to 0.5 cd/A . Because the voltages needed for conduction are so high the power efficiency is only $25 \times 10^{-3} \text{ lm/W}$ for the 5% diode and $50 \times 10^{-3} \text{ lm/W}$ for the 10% diode.

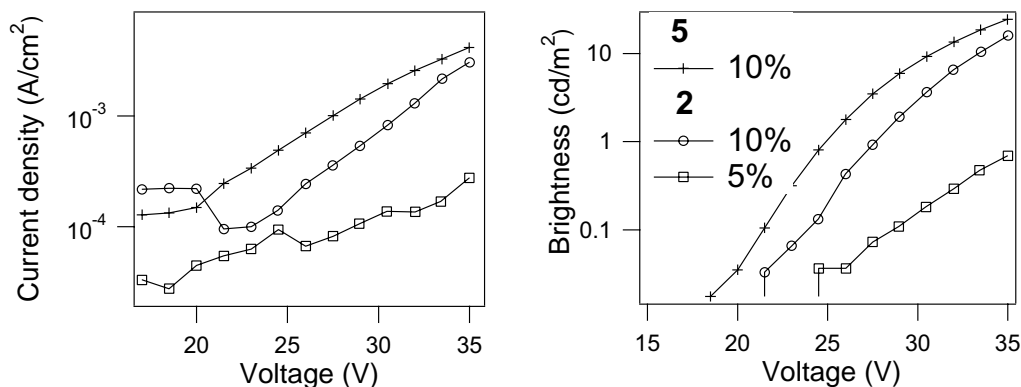


Figure 6. Current density (left) and brightness (right) of PS diodes containing 5% of **2** (open squares), 10% **2** (open circles) and 10% **5** (crosses).

From Figure 4 it is predicted that, when the D-b-A molecules are embedded in a non-conducting matrix like PS, conduction and electroluminescence can only be expected at concentrations that allow a closed path of contacting D-b-A molecules to be established between anode and cathode, that is, above the so-called percolation limit. That the loading concentration has to be raised in PS to obtain reasonable currents is thus typical for such percolation behaviour, and was previously found for PS films containing a p-phenylene vinylene trimer as well.²³ However, with that system Frederiksen et al. had to increase the loading concentration to over 15% to obtain diode-like behaviour with a turn-on voltage of over 30 V (light-output was not quantitatively measured). Increasing the concentration of **2** indeed directly leads to higher currents through the layer as the mean molecular separation of the D-b-A molecules gets smaller. Interestingly also the efficiency in cd/A increases going from 5% to 10% loading concentration of **2** in PS. This is partly due to the accompanying red-shift of the luminescence (see Figure 7 and discussion below) that produces a larger overlap of the emission with the eye sensitivity curve. However, also the efficiency expressed in photons/electrons goes up from 0.15% to 0.25%. In terms of the mechanism depicted in Figure 4 this suggests that the ratio of the charge recombination current due to intramolecular radiative recombination on the one hand and the sum of other current supporting processes on the other hand (i.e., the intermolecular dark recombination, also shown in Figure 4, as well as the transport between the electrodes of holes via D moieties and of electrons via A moieties, pathways not shown in Figure 4) shifts to favor the former at higher doping concentrations.

The diode containing 10% of **5** displays a lower turn-on voltage for light (*circa* 20 V) than the diode with 10% of **2**, however the maximum efficiency of 0.6 cd/A is very comparable to that of **2**, as are the photoluminescent quantum yields of both systems. The brightness and efficiency (especially the power efficiency, due to the high turn-on voltage) that are reached in these diodes are still very low, even for a blue diode.

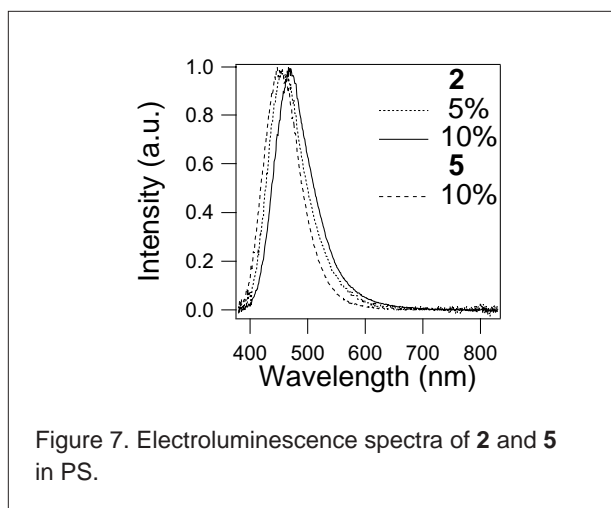


Figure 7. Electroluminescence spectra of **2** and **5** in PS.

The spectral distribution (see Figure 7) of the electroluminescence is voltage independent and closely matches the photoluminescence of the films, showing that indeed emission occurs from the CT state. The diode containing 10% of **5** displays emission with a maximum positioned at 451 nm, the one containing 5% of **2** at 456 nm and 10% at 464 nm. The red shift of the CT fluorescence with increasing concentration signals that at higher concentration the D-b-A molecules experience a more polar/polarisable environment as compared to that experienced in pure polystyrene. This clearly signals the neighbourhood of other D-b-A molecules.

Although all PS based devices degrade visibly, the shape of the electroluminescent spectrum remains unchanged during operation. Typically the brightness reduces drastically during operation of a few minutes (see below for more details on device degradation).

D-b-A Doped Poly(9-vinylcarbazole) Diodes

Although the production of electroluminescence from D-b-A molecules at high concentration in a non-conducting matrix like PS described in the previous section serves as a nice proof of principle it is clear from the very high voltages required and the low brightness achievable that a semiconducting polymer matrix might be preferable especially to lower the turn-on voltage of the diode by facilitating charge-injection and/or charge-transport. Because our main goal was to create a blue emitting diode, the choice of such a polymer is, however, very limited. Most semiconducting polymers contain large conjugated systems that have excitation energies below the photon energy of blue light and will therefore quench the CT excited state of our D-b-A systems by energy transfer. Others, that have higher excitation energies, quench by electron transfer because they are either stronger donors or stronger acceptors than the D and A units incorporated in our D-b-A systems. However, the well known hole-conducting material poly(9-vinylcarbazole) (PVK) has a high excitation energy (typically above 3.2 eV) and its carbazole chromophore is a significantly weaker electron donor than the aniline units in our D-b-A systems. As expected, use of PVK instead of PS substantially increased the device performance. Films of PVK were prepared by spincoating 15 mg/ml toluene solutions at a speed of 1500 rpm to yield 70 nm films. In all diodes barium covered with aluminium was used as the cathode, which lowers the turn-on voltage of the devices substantially as compared to aluminium alone.

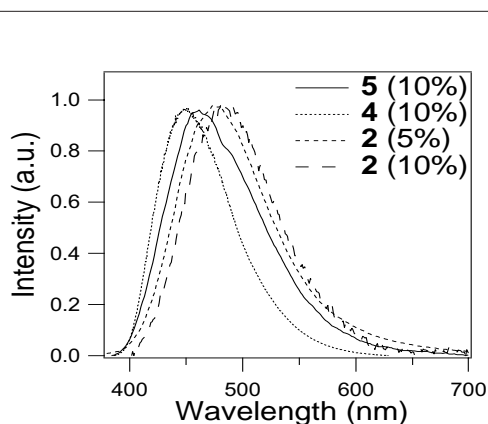


Figure 8. Electroluminescence spectra of PVK diodes containing the DbA systems **5** (continual line), **4** (dotted line) and **2** (dashed lines).

PVK diodes that were doped with one of the D-b-A compounds **2**, **4**, or **5** display bright blue to greenish electroluminescence depending on the compound and its concentration. It should be noted that PVK itself is fluorescent at shorter wavelength than **2**, **4**, and **5** and also displays very weak electroluminescence. However, doping with the D-b-A systems used fully quenches the PVK emission. In Table 2 the EL maxima are listed for diodes containing 5% and 10% of **2**, **4**, and **5**, while the spectra are shown in Figure 8. Especially for 10% of **2** the position of the maximum has red-shifted so much that this diode appears green to the eye.

When looking at the initial performance (Figure 9) it can be said that the turn-on voltages for light of the blue D-b-A /PVK diodes (approx. 6.5 V) are significantly lower than for the diodes with PS (above 20 V), and that with PVK as the matrix a brightness one to two orders above that of the PS based diodes can be achieved.

Table 2. Position of the electroluminescence maxima (in nm) of PVK diodes containing 5% or 10% of **2**, **4**, or **5**.

	2	4	5
5 %	475	450	455
10 %	485	455	460

Furthermore it shows from Figure 9, that for a blue diode system **5** displays by far the best performance in terms of light output. The same holds true for the maximum power efficiency, which is reached at 10 V in all diodes and amounts to 0.06 lm/W for **5**, 0.03 lm/W for **4** and 0.01 lm/W for **2**. Though the absolute amount of light coming from the PVK diodes is substantially higher than from the PS diodes, the power efficiencies are very comparable. This is a result of the efficiencies expressed in cd/A or photons/electrons being about a factor 3 lower in PVK diodes, whereas the turn-on voltage is about a factor 3 higher in polystyrene. Clearly charge transport is much easier in the PVK than in the PS based diodes. PVK, however, while it has a high mobility for holes, is a very poor electron conductor. Thus only the hole mobility is enhanced while the electron transport still is limited to the hopping mechanism via A units of the D-b-A molecules (see Figure 4). As a result the recombination of charges occurs much closer to the metal cathode in the PVK diodes than in the PS diodes and the electroluminescence is thereby more subject to the quenching action of the metal. This probably contributes to the lower cd/A efficiency of the PVK diodes.

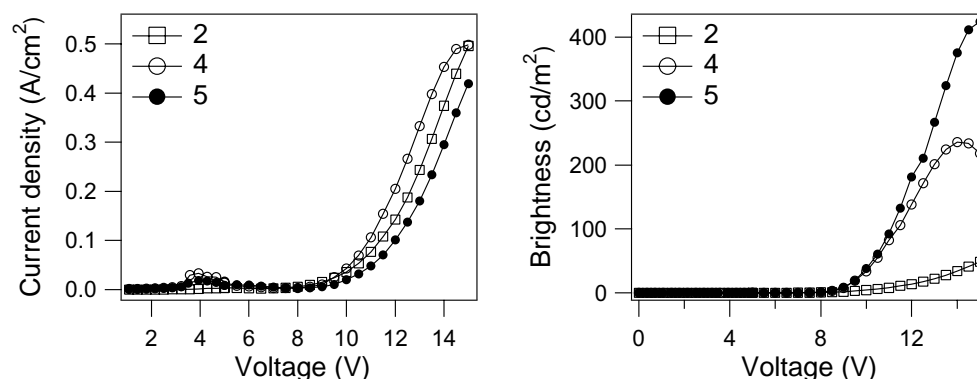


Figure 9. Current density (left) and brightness (right) of PVK diodes containing **2** (5%), **4** (10%) and **5** (10%).

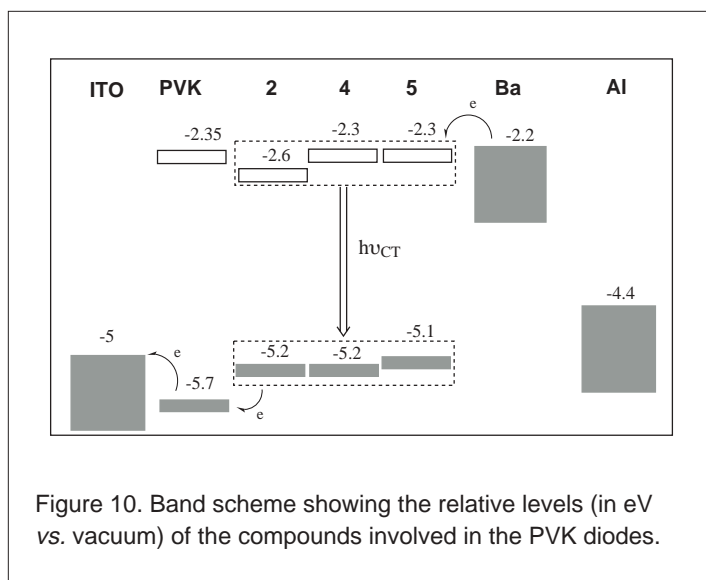


Figure 10. Band scheme showing the relative levels (in eV vs. vacuum) of the compounds involved in the PVK diodes.

positions of the HOMOs are better reproduced in the scheme, considering that the oxidation potential of *N*-methylcarbazole is around 1–1.1 V²⁶ as compared to 0.7 V (in acetonitrile vs SCE) for the *N,N*-dialkylaniline donor in the D-b-A systems used. Hence, the positive charge will not remain trapped on PVK but will be transferred to the D-b-A donor.

The difference that arises between the efficiency of **5** and **4** can again only partially be attributed to the fact that the emission of **5** overlaps more strongly with the photopic efficacy curve as it is somewhat red-shifted as compared to **4**. In addition, however, the fact that **5** contains a somewhat stronger donor than **4** may allow it to act as more efficient hole trap with respect to PVK, thus also leading to light emission occurring closer to the ITO electrode where the quenching action of the metal electrode is not felt. The main cause for the relatively poor performance of **2** lies in the lower doping concentration that is used with this compound in order to maintain a blue emission from the diode. As a result there are less recombination centres present that can act as a charge trap.

Hole-only devices of PVK with **2** and **5**

A number of devices were constructed that contain gold as the cathode instead of barium/aluminium. In this way a so-called “hole-only” device is formed that does not emit light but only allows holes to flow through the device. The thickness of the PVK film is the same in both the diodes and the hole-only devices. The current densities in the LEDs (thus with Ba/Al, referred to as double carrier) are considerably higher than in these hole-only devices, because in the double carrier devices also electrons— injected in the diode—that capture holes contribute to the current (recombination current). From the current density in the hole-only devices an estimation can be made of the barrier height for hole-injection using the Fowler-Nordheim field-emission tunnelling theory.²⁷ For this it is assumed that the “hole” tunnels through a triangular barrier from the electrode into the film.

$$J = F^2 \exp \left[\frac{-8\pi}{3hF} \sqrt{m^*} (\phi_b)^{3/2} \right] \quad [5]$$

In eq [5], J represents the current density, F the field, m^* the effective mass of the charge carrier and ϕ_b the height of the barrier. If a plot is made of the logarithm of the current density divided by the squared field versus the reciprocal field, a fairly linear curve is found above the turn-on field. From the slope then follows the barrier height if we take for m^* the free electron mass. For the devices with **2** and **5** the slopes yield a barrier of respectively 0.51 eV and 0.49 eV, very comparable to the barrier found for a non-doped (PVK) hole-only device (0.46 eV), which itself is in range with the barrier between ITO and PVK, estimated from the band scheme (0.7 eV, see Figure 10). This implies that the addition of the D-b-A dopant does not significantly change the barrier for hole-injection from the ITO and that also in the D-b-A doped devices the major part of the holes is primarily injected into PVK. That direct hole injection into the D-b-A molecule is not important also receives support from the fact that the current does not display space-charge limited behaviour. This behaviour would have occurred when there is no barrier for charge injection (which is

In Figure 10 the relative positions are shown of the redox levels of the compounds used. The work functions of the metals, of ITO and of PVK are taken from literature,²⁴ the other are indirectly placed versus the vacuum level by positioning them relative to the oxidation potential of ferrocene (–4.8 V vs vacuum), which also corresponds to the statement of de Leeuw et al.²⁵ that the solid state ionisation potential equals the electrochemical potential (vs SCE) +4.4 V. From the band scheme in Figure 10 it becomes immediately clear that barium is an optimal electron injecting electrode for the devices. It remains questionable to compare the levels of PVK with that of the D-b-A systems—they were not obtained by the same method—especially regarding the position of the LUMO. We believe that vinylpyrene is a better electron acceptor than *N*-vinylcarbazole, which is not reflected by the relative position of the unoccupied levels of PVK and **4/5** in the scheme. The relative

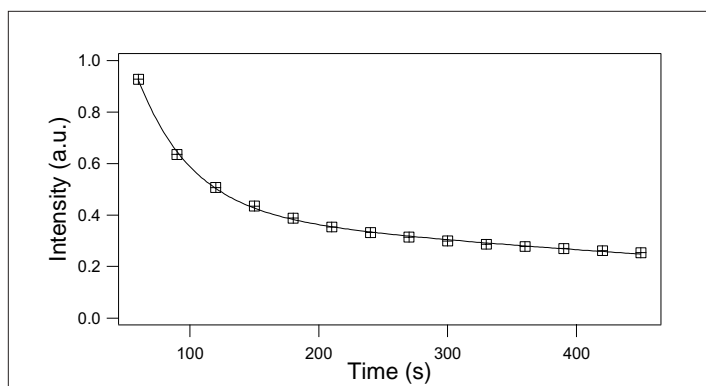


Figure 11. Decay of the electroluminescence intensity during continuous operation of a **2**/PVK diode at 10 V.

It can be seen from Figure 11 that especially during the first two minutes of operation at a constant low voltage (10 V), the decrease in light intensity is large. During longer operation of the diode, the decline of the intensity diminishes. This initial decay is common to PLEDs. Various degradation mechanisms have been proposed for PLEDs which include: a reaction with traces of oxygen, a reaction with both cathode and anode, and migration of the low molecular weight components. It cannot be excluded that the replacement of the aluminium cathode by barium has resulted in a more efficient device, but also enhanced the reactivity at the metal electrode. Another explanation for the fast degradation in these systems may be the reactivity of the donor radical cation (*N,N*-dialkylaniline in all systems studied). In cyclic voltammetry studies of **2** it shows that in solution the one electron oxidation of the donor in the system is irreversible, indicating that the donor radical cation is susceptible to degradation. In fact, degradation of the radical cations of tertiary amines and *N,N*-dialkylarylamines is well documented. It involves a series of events that in general starts with proton loss from an α -C atom, but ultimately also leads to C-N fission (i.e., dealkylation).^{28,29}

Concluding Remarks

Electrogeneration of the intramolecular CT fluorescence of the donor-bridge-acceptor systems **2**, **4**, and **5** occurs readily in polymer films. This is not only the case in a hole conducting polymer like PVK but even in a strongly insulating polymer like PS. In the PVK diodes the hole-injection occurs primarily into PVK. However, the positive charge will be trapped on the D-b-A molecule, as is evident from the band scheme (Figure 10). Because of the very poor electron conducting properties of PVK electron injection at the cathode side occurs into the D-b-A molecules. In PS it appears that both hole-injection and electron-injection occur directly in the D-b-A molecules residing close to the anode and the cathode respectively. Either way—be it *via* the polymer or via direct injection—eventually oxidation of the D-b-A donor moiety and reduction of the acceptor moiety takes place. Degenerate charge hopping between neighbouring molecules then occurs until a “hole” and “electron” reside on the same molecule, which is equivalent to formation of the CT excited state, that finally relaxes by intramolecular charge recombination under the emission of CT fluorescence. It appears to be a rather unique property of the present devices, as compared to other electroluminescent systems, that the charge recombination itself is the emissive process. This implies that the electrochemical level is also the emissive level in contrast to the more usual situation where the energy liberated in charge recombination leads to population of an emissive state of lower energy. The fact that here the CT state itself is the emitter, without the need for further energy wastage to populate a lower energy emissive state of localized nature, is probably the reason why blue emission can readily be produced in these LEDs. Furthermore it has been found that with PVK as a matrix very bright blue electroluminescence can be produced. Especially with **5** as the emitter a brightness above 400 cd/m² has been realised (see Figure 9), which readily matches the brightness (ca. 100 cd/m²) of TV screens. It must be noted, however, that as yet the operational stability of the D-b-A based PLEDs is very limited. Thus, before applications can be considered, major improvements will be required in the device design (i.e., addition of protective layers) and especially in the stability of the D-b-A systems towards breakdown upon one electron oxidation and reduction.

implied by the small difference between the levels of ITO and the D-b-A systems) and would have resulted in a quadratic dependence of the current density on the voltage. This was not the case for any of the hole-only devices measured.

Device (in)stability

Although much effort was put in the exclusion of water and air from the diodes during the measurements, which generally enhances the lifetime of the LEDs, it still turned out that the devices are prone to fast degradation during operation. Also the efficiency of the device goes down and the position of the maximum efficiency appears to shift somewhat to higher voltage too. In subsequent cycles after the first one the light output gradually decreases further.

References

1. Closs, G. L.; Miller, J. R. *Science* **1988**, *240*, 440.
2. Verhoeven, J. W. In *Advances in Chemical Physics, Electron Transfer - From Isolated Molecules to Biomolecules, Part One*; Jortner, J., Bixon, M., Eds.; John Wiley & Sons, 1999; Vol. 106, pp 603.
3. Wasielewski, M. R. *Chem. Rev.* **1992**, *92*, 435.
4. Hoffmann, R.; Imamura, A.; Hehre, W. J. *J. Am. Chem. Soc.* **1968**, *90*, 1499.
5. Oliver, A. M.; Paddon-Row, M. N.; Kroon, J.; Verhoeven, J. W. *Chem. Phys. Lett.* **1992**, *191*, 371.
6. Pasma, P.; Rob, F.; Verhoeven, J. W. *J. Am. Chem. Soc.* **1982**, *104*, 5127.
7. Dekkers, A. W. J. D.; Verhoeven, J. W.; Speckamp, W. N. *Tetrahedron* **1973**, *29*, 1691.
8. Lilichenko, M.; Tittelbach-Helmrich, D.; Verhoeven, J. W.; Gould, I. R.; Meyers, A. B. *J. Chem. Phys.* **1998**, *109*, 10958.
9. Mes, G. F.; deJong, B.; vanRamesdonk, H. J.; Verhoeven, J. W.; Warman, J. M.; DeHaas, M. P.; HorsmanVanDeDool, L. E. W. *J. Am. Chem. Soc.* **1984**, *106*, 6524.
10. Goes, M.; Lauteslager, X. Y.; Verhoeven, J. W.; Hofstraat, J. W. *Eur. J. Org. Chem.* **1998**, 2373.
11. Wegewijs, B.; Verhoeven, J. W. In *Advances in Chemical Physics, Electron Transfer - From Isolated Molecules to Biomolecules, Part One*; Jortner, J., Bixon, M., Eds.; John Wiley & Sons, Inc., 1999; Vol. 106, pp 221.
12. Hermant, R. M.; Bakker, N. A. C.; Scherer, T.; Krijnen, B.; Verhoeven, J. W. *J. Am. Chem. Soc.* **1990**, *112*, 1214.
13. Bartels, M. J.; Koeberg, M.; Verhoeven, J. W. *Eur. J. Org. Chem.* **1999**, 2391.
14. vanRamesdonk, H. J.; Vos, M.; Verhoeven, J. W.; M'hlman, G. R.; Tissink, N. A.; Meesen, A. W. *Polymer* **1987**, *28*, 951.
15. Verhey, H. J.; Gebben, B.; Hofstraat, J. W.; Verhoeven, J. W. *J. Polym. Sci.: Part A: Polym. Chem.* **1995**, *33*, 399.
16. Verhey, H. J.; Hofstraat, J. W.; Bekker, C. H. W.; Verhoeven, J. W. *New J. Chem.* **1996**, *20*, 809.
17. Verhey, H. J.; vanderVen, L. G. J.; Bekker, C. H. W.; Hofstraat, J. W.; Verhoeven, J. W. *Polymer* **1997**, *38*, 4491.
18. Goes, M.; deGroot, M.; Koeberg, M.; Verhoeven, J. W.; Lokan, N. R.; Shephard, M. J.; Paddon-Row, M. N. *J. Phys. Chem. A* **2002**, *106*, 2129.
19. Marcus, R. A. *J. Phys. Chem.* **1989**, *93*, 3078.
20. Goes, M. Photo- and Electroluminescence Generated by Intramolecular Charge Transfer. Ph.D. Thesis, University of Amsterdam, 2002.
21. Bakker, B. H.; Goes, M.; Hoebe, N.; vanRamesdonk, H. J.; Verhoeven, J. W.; Werts, M. H. V.; Hofstraat, J. W. *Coord. Chem. Rev.* **2000**, *208*, 3.
22. Scherer, T.; Hielkema, W.; Krijnen, B.; Hermant, R. M.; Eijkelhoff, C.; Kerkhof, F.; Ng, A. K. F.; Verleg, R.; Tol, E. B. v. d.; Brouwer, A. M.; Verhoeven, J. W. *Recl. Trav. Chim. Pays-Bas* **1993**, *112*, 535.
23. Frederiksen, P.; Bjørnholm, T.; Madsen, T.; Bechgaard, H. G. *J. Mater. Chem.* **1994**, *4*, 675.
24. Wang, J.; Kawabe, Y.; Shaheen, S. E.; Morell, M. M.; Jabbour, G. E.; Lee, P. A.; Anderson, J.; Armstrong, N. R.; Kippelen, B.; Mash, E. A.; Peyghambarian, N. *Adv. Mater.* **1998**, *10*, 230.
25. deLeeuw, D. M.; Simenon, M. M. J.; Brown, A. R.; Einerhand, R. E. F. *Synth. Met.* **1997**, *87*, 53.
26. Wheland, R. C.; Gillson, J. L. *J. Am. Chem. Soc.* **1976**, *98*, 3916.
27. Fowler, R. H.; Nordheim, L. *Proc. Roy. Soc. (London)* **1928**, *119A*, 173.
28. Gaillard, E. R.; Whitten, D. G. *Acc. Chem. Res.* **1996**, *29*, 292.
29. Parker, V. D.; Tilset, M. *J. Am. Chem. Soc.* **1991**, *113*, 8778.

About the Authors

Jan W. Verhoeven received his Ph.D. from the University of Amsterdam in 1969 under the guidance of Thymen J. de Boer. After a brief postdoctoral period with Robert Schwyzer at the ETH in Zürich he returned to the University of Amsterdam. From 1979 until the end of 2001 he was full professor in physical organic chemistry studying mainly photoinduced electron transfer and luminescent materials. He is now an emeritus professor at the Laboratory of Organic Chemistry, University of Amsterdam, Nieuwe Achtergracht 129, 1018 WS Amsterdam, The Netherlands; email: jwv@science.uva.nl.

Marijn Goes received his M.Sc. degree in 1998 from the University of Amsterdam with research in the field of development of luminescent labels for polymer probing. He continued at the same university, which resulted in a Ph.D. degree in 2002 after research of photo- and electroluminescent processes generated by intramolecular charge transfer.

Hans Hofstraat received his Ph.D from the Free University, Amsterdam. Subsequently, he was a postdoc at the ETH in Zürich. From 1987 he worked as head of the Department of Chemical Physics in the laboratory of the Dutch Public Works Department, developing laser techniques for the study of the marine environment. In 1991 he joined Akzo Nobel Central Research in Arnhem, The Netherlands, where he was responsible for research in the areas of optical spectroscopy, photonic polymers and diagnostics. He left Akzo Nobel for Philips in 1998. Currently, he is head of the Department of Polymers and Organic Chemistry in the Philips Research Laboratories in Eindhoven, The Netherlands. Since 1998 he is part-time professor in the Institute of Molecular Chemistry of the University of Amsterdam, focusing on Applications of Molecular Photonic Materials.

Klemens Brunner completed his M.Sc. at the University of Vienna with a master's thesis on polymer layers on surface acoustic wave devices. During his studies he was a participant in the Joint Study Program at the University of California at Berkeley and did research in the research group of Prof. Dr. Andrew Streitwieser, College of Chemistry, on transition state complexes. After his masters he joined the research group of Prof. Dr. H. F. Kauffmann as scientific employee and graduated from the University of Vienna in the field of ultra short-time spectroscopy of disordered materials. He joined Philips Research in 1999 and is working since then in the Polymers and Organic Chemistry group. The main focus is on the characterization and optimization of novel electroluminescent materials in polymer light emitting diodes. His address is Philips Research Laboratories Eindhoven, WB 623, Prof. Holstlaan 4, 5656 AA Eindhoven, The Netherlands; email: klemens.brunner@philips.com.

Technical Note

SLM 48000 Spectrofluorimeter Non-Volatile Memory IC Replacement

David Kessel

Department of Pharmacology, Wayne State University School of Medicine

One of the premiere fluorescence instruments from the 1980s was the SLM 48000 series fluorometer. This device can determine emission and excitation spectra, polarization and lifetimes (by the frequency domain method). If fitted with a second monochromator, fluorescence polarization studies can be automated, using a reference standard and a sample compartment turret rotator. The turret is also used to automate lifetime acquisitions. Unfortunately, parts for the 48000 are becoming unavailable. Maintenance of SLM instruments has been sequentially passed along to other organizations with a limited interest or ability for providing parts and advice. Olis Inc (olis@negio.net) will rebuild an SLM 48000 for \$30,000—retaining the optics and monochromators, while upgrading the electronics to a Windows NT compatible system. Our instrument, upgraded in 1984 with 5-phase motors and a rotating turret assembly, appears to be in good working order, but we recently experienced a failure in the non-volatile RAM IC designed to maintain the monochromator settings when the power is off, using an internal battery. This IC is found on the CPU board in a special mount; IC18 on the circuit diagram. The original part number was E-1445, originally sold by Mostek, an Indian organization. The equivalent from current inventory is the DS1220AB, a non-volatile SRAM from Dallas Semiconductor. Dallas prefers to sell these in lots of 1000, but a single IC can be obtained from Newark Electronics (Newark.com), catalog No. 06F4220 @ \$14.56 + shipping. These ICs are said to be usable for 10 years, and the lithium battery is enabled only after power is first applied.

While maintaining operation of an instrument from the 1980s is likely best accomplished by using the Olis Inc. upgrade, a user needing only a non-volatile memory IC could defer the upgrade by simply replacing this SRAM device. We may have additional advice on SLM maintenance if anything else fails.

Dr. Kessel's email address is dhkessel@med.wayne.edu.

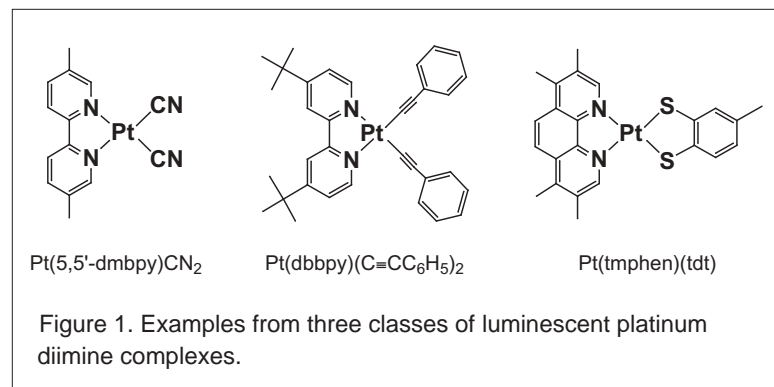
Cross-quenching Investigations of Platinum(II) Diimine Complexes

Wendi L. Fleeman and William B. Connick
University of Cincinnati

Introduction

There is growing interest in square planar platinum(II) diimine complexes as environmental probes for chemical sensing applications.^{1,2} The open coordination sites around the metal center in these compounds suggest that molecular properties, such as absorption and emission of light, may be significantly perturbed by interactions with the surrounding medium. This notion and other possible applications have inspired investigations aimed at elucidating the factors governing the electronic structures of these chromophores.³⁻⁶ Such studies have established that neutral platinum(II) diimine complexes exhibit rich spectroscopic and photophysical properties, including in some cases room-temperature fluid solution emission originating from a long-lived predominantly triplet excited state (>100 ns).

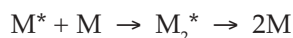
The orbital character of the lowest emissive excited state depends on the nature of the anionic ancillary ligands (Figure 1). In the case of cyanide groups, the colorless compounds (e.g., Pt(5,5'-dmbpy)(CN)₂) exhibit green emission characteristic of a ligand-centered ³(π-π*) excited state. Substitution with phenyl acetylide groups results in yellow complexes (e.g., Pt(dbbpy)(C≡CC₆H₅)₂) with orange or red emission characteristic of a spin-forbidden metal-to-ligand charge transfer state. In the case of dithiolate ligands such as 1,2-toluenedithiolate, the red-violet compounds (e.g., Pt(tmphen)(tdt)) exhibit solvent-sensitive



red to near infrared emission. The observed emission is characteristic of a lowest excited state having significant dithiolate-to-diimine charge transfer character, often identified as a metal-mixed-ligand-to-ligand charge transfer state (MMLLCT). Thus, by varying the nature of the ancillary ligands, it is possible to tune the excited-state energies of these complexes from approximately 1.7 to 2.8 eV.⁷

Self-Quenching Reactions

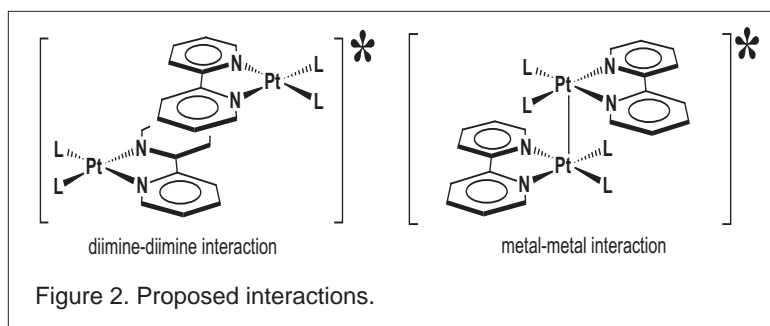
As early as 1989, Che and coworkers recognized that the emission lifetime of Pt(5,5'-dmbpy)(CN)₂ is concentration dependent.⁸ The observed behavior is consistent with an excited-state self-quenching reaction in which an excited platinum complex (M*) reacts with a ground-state complex (M) to form an excimer (M₂*):



The excimer rapidly relaxes to give two ground-state complexes and the stored light energy is squandered as heat. The observed rate of emission decay (k') was found to decrease linearly with concentration, corresponding to a rapid self-quenching reaction ($k_{sq} = 4.8 \times 10^9 \text{ M}^{-1}\text{s}^{-1}$):

$$k' = k_i + k_{sq}[\text{Pt}] \quad (1)$$

Since this earliest observation, several groups^{1,9-12} have noted similar self-quenching behavior for other complexes. In all cases, the self-quenching rates are nearly diffusion limited, ranging from 10^9 to $10^{10} \text{ M}^{-1}\text{s}^{-1}$. In several instances, emission from the excimer was observed.^{9,12,13} However, it was not until 1999 that Eisenberg and coworkers established that self-quenching is a general phenomenon, characteristic of all fluid-solution emitting platinum(II) diimine



complexes, regardless of the lowest emissive triplet excited state of the compound.¹⁴

Because self-quenching presents serious practical problems for applications demanding a long-lived excited state in fluid solution, there is considerable interest in understanding and learning to control this behavior. At present, the structure of the excimer is not known, and the exact nature of the stabilizing intermolecular interactions is uncertain. Both (i) diimine-diimine interactions

and (ii) metal-metal interactions have been proposed to play a role in excimer formation (Figure 2).^{1,10,12,15} Indeed, these interactions occur in crystals and solution aggregates of these complexes,^{3,11,16-19} making it difficult to predict which mode of association will dominate excited-state association. While direct characterization of the excimer seems an attractive approach to answering these questions, these experiments are hampered by the apparent short lifetimes and low emission quantum yields of the excimers as compared to those of monomers. Moreover, poor solubility of the monomers and possible ground-state aggregation at higher concentrations has precluded measurements over a wide range of concentrations.

Cross-Quenching

The preceding considerations have led us to investigate cross-quenching reactions as an indirect means of elucidating the mechanism of association. A cross-quenching reaction is similar to its self-quenching counterpart with the distinction that the excited monomer, M^* , reacts with a different ground-state complex, Q , presumably to form an exciplex, MQ^* :



This approach enables us to probe the photophysical behavior of a single chromophore in the presence of a wide variety of possible quenchers (Q).

A series of cross-quenching reactions of $Pt(tmphen)(tdt)$ has been characterized by steady-state and time-resolved emission spectroscopies. Advantages of this chromophore include a low-energy emissive excited state ($E_{0,0}=2.1\text{eV}$), a relatively high quantum yield (0.6%), and a long emission lifetime ($\tau=1/k_1=1911\text{ ns}$; $\lambda_{\text{max}}=720\text{ nm}$). In addition, the UV-visible absorption spectrum of the complex exhibits a low-energy intense band ($\lambda_{\text{max}}=535\text{ nm}$, CH_2Cl_2), allowing for selective excitation. Appropriate quenchers for cross-quenching studies were selected based on solubility, energetics ($E_{0,0}>2.1\text{eV}$), and thermal inertness to the chromophore. In addition, neutral quenchers were chosen to avoid complications associated with variations in ionic strength.

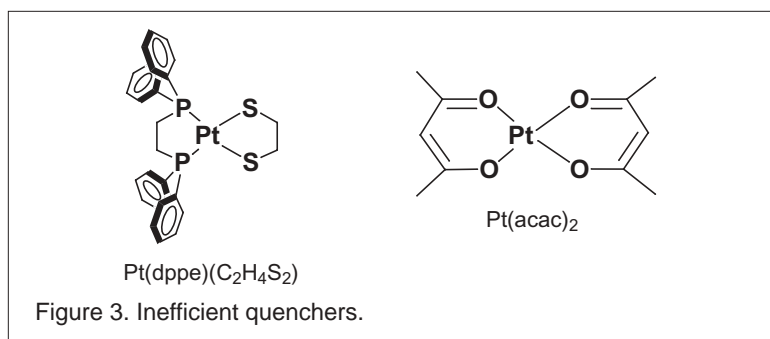
Cross-quenching was assessed by monitoring the decrease in the emission intensity of $Pt(tmphen)(tdt)$ in degassed methylene chloride with increasing quencher concentration. The ratio of the emission quantum yield in the absence (Φ_0) and presence (Φ) of quencher was found to depend linearly on the concentration of added quencher, $[Q]$, according to:

$$\Phi_0/\Phi = 1 + k_{\text{cq}}/[Q]k' \quad (2)$$

where k_{cq} is the bimolecular cross-quenching rate constant. In several instances, the results of these steady-state measurements have been corroborated by time-resolved experiments in which the emission lifetime (τ_{obs}) of the chromophore was determined in the absence and presence of quencher. The rate of $Pt(tmphen)(tdt)$ emission decay ($k''=1/\tau_{\text{obs}}$) was found to depend linearly on the concentration of added quencher according to:

$$k'' = k_{\text{cq}}[Q] + k' \quad (3)$$

The values of k_{cq} obtained from steady-state and time-resolved measurements are in good agreement, indicating that ground-state aggregation does not play a dominant role in quenching under these conditions.²⁰



Cross-quenching Investigations

In order to assess which interactions are important for quenching, we have selected quenchers that will allow for specific intermolecular interactions, while precluding others. For example, in order to probe the role of diimine-diimine interactions, the emission intensity of Pt(tmphen)(tdt) was monitored in the presence of varying concentrations of 1,10-phenanthroline (phen), naphthalene,¹⁴ 2,2'-bipyridine (bpy), and 4,4'-bipyridine.⁷ These organic aromatics and nitro-

gen-based nucleophiles have negligible effect on the Pt(tmphen)(tdt) emission intensity and lifetime, indicating they are ineffective quenchers.

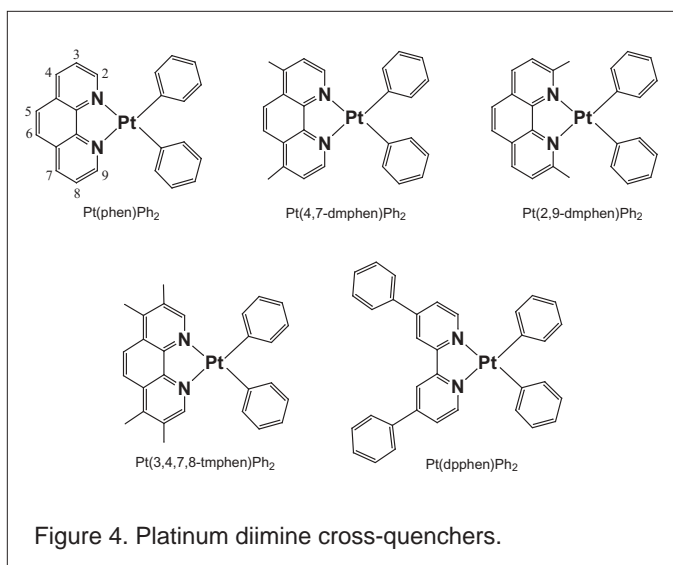
Platinum complexes lacking a diimine ligand were chosen to investigate the role of intermolecular Pt-Pt interactions in quenching (Figure 3).⁷ No quenching ($<10^6 \text{ M}^{-1}\text{s}^{-1}$) of the Pt(tmphen)(tdt) emission was observed upon addition of Pt(dppe)(C₂H₄S₂) up to concentrations of 10^{-2} M . Addition of a large excess of Pt(acac)₂ ($1.5 \times 10^{-2} \text{ M}$) to a solution of Pt(tmphen)(tdt) results in a slight, but discernible decrease in emission intensity, not attributable to irreversible photochemistry. Although the metal center of Pt(acac)₂ is relatively accessible, the corresponding cross-quenching rate ($<10^7 \text{ M}^{-1}\text{s}^{-1}$) is slow compared to self-quenching rates.

In fact, rapid quenching (10^9 - $10^{10} \text{ M}^{-1}\text{s}^{-1}$) was only observed for complexes containing both a diimine and a platinum center.^{7,14} We have synthesized and characterized a series of Pt(II) diimine quenchers with varying steric and electronic properties (Figure 4). For each quencher the diimine was either a substituted 2,2'-bipyridine or 1,10-phenanthroline ligand (e.g., methyl, *t*-butyl, phenyl). The ancillary anionic ligands were chloride, phenyl, or mesityl groups. In the presence of these quenchers, the emission intensity of Pt(tmphen)(tdt) was found to obey Stern-Volmer kinetics according to equation 2. Representative plots are shown in Figure 5 and Figure 6 along with the cross-quenching rates, ranging from 0.2 - $8.0 \times 10^9 \text{ M}^{-1}\text{s}^{-1}$ (Table 1).

Table 1. Cross-quenching data of Pt(tmphen)(tdt) emission in CH₂Cl₂.

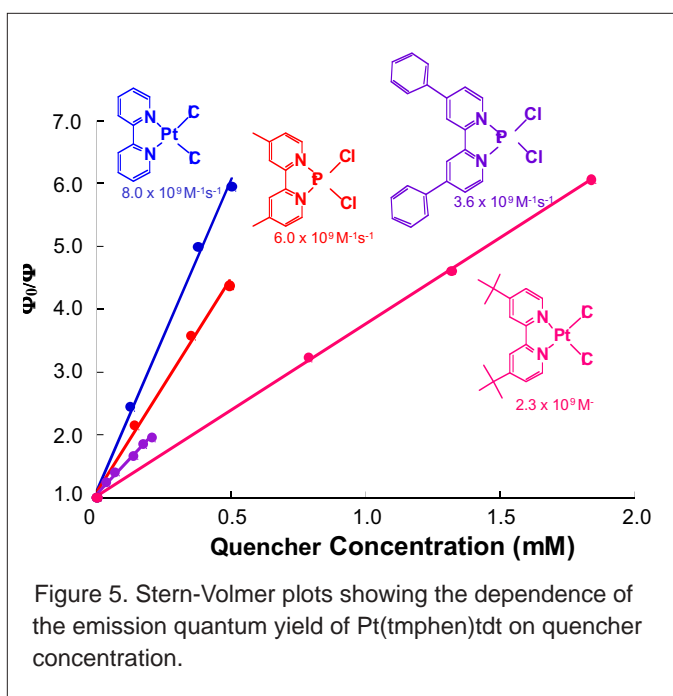
Quencher	$k_{\text{eq}} \cdot 10^9 \text{ M}^{-1}\text{s}^{-1}$
Pt(bpy)Cl ₂	8.0 ^a
Pt(dmbpy)Cl ₂	6.0 ^a
Pt(dpbbpy)Cl ₂	3.6 ^a
Pt(dbbpy)Cl ₂	2.3 ^a , 2.1 ^{b,c}
Pt(bpy)Ph ₂	3.7 ^a
Pt(phen)Ph ₂	4.3 ^a
Pt(4,7-dmphen)Ph ₂	4.3 ^a
Pt(3,4,7,8-tmphen)Ph ₂	4.2 ^{a,b}
Pt(2,9-dmphen)Ph ₂	2.3 ^a
Pt(dpphen)Ph ₂	2.6 ^a
Pt(dbbpy)(CN) ₂	0.9 ^{b,c}
Pt(bpy)(Mes)Cl	0.2 ^{a,b}
Pt(acac) ₂	<0.01 ^{a,d}
Pt(dppe)(C ₂ H ₄ S ₂)	<0.001 ^{a,d}
2,2'-bipyridine	<0.001 ^{a,d}
4,4'-bipyridine	<0.001 ^{a,d}
naphthalene	<0.001 ^{a,d}
phenanthroline	<0.001 ^{a,d}

^aFrom steady-state emission measurements. ^bFrom emission decay rate measurements. ^cRef 14. ^dNo quenching was observed, and this value represents the experimental detection limit.



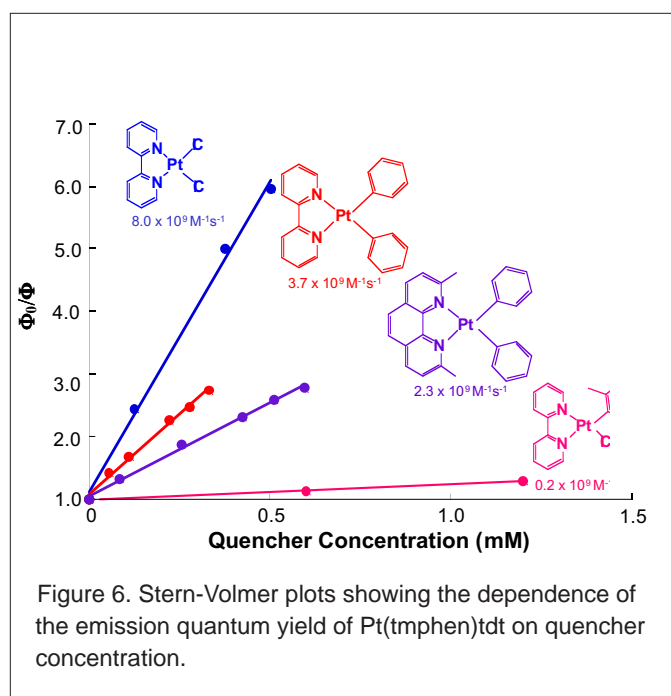
$k_{\text{cq}} = 4.3 \times 10^9 \text{ M}^{-1}\text{s}^{-1}$; Pt(4,7-dmphen) Ph_2 , $k_{\text{cq}} = 4.3 \times 10^9 \text{ M}^{-1}\text{s}^{-1}$; Pt(3,4,7,8-tmphen) Ph_2 , $k_{\text{cq}} = 4.2 \times 10^9 \text{ M}^{-1}\text{s}^{-1}$). In contrast, methylation at the 2 and 9 positions of phenanthroline causes a significant decrease in the rate of quenching. In fact, the observed rate of quenching for Pt(2,9-dmphen) Ph_2 ($k_{\text{cq}} = 2.3 \times 10^9 \text{ M}^{-1}\text{s}^{-1}$) is slower than that of Pt(dpphen) Ph_2 ($k_{\text{cq}} = 2.6 \times 10^9 \text{ M}^{-1}\text{s}^{-1}$). The crystal structure of Pt(2,9-dmphen) Ph_2 shows that steric demands of the methyl groups result in large distortions relative to the geometry of Pt(phen) Ph_2 . The dihedral angle formed by the best fit plane for the diimine N=C-C=N atoms and the plane defined by the Pt center and two bonded carbon atoms is 31° .²¹ This distortion is anticipated to inhibit intermolecular diimine-diimine interactions, as well as Pt-Pt interactions. In addition, the methyl groups can be expected to protect the platinum center and restrict rotation of the phenyl ligands, further inhibiting close approach of two platinum complexes.

Increasing steric bulk near the quencher metal center also results in less efficient quenching (Figure 6). Replacing two chloride ligands with two phenyl ligands causes a nearly two-fold decrease in the rate of quenching (e.g., Pt(bpy) Cl_2 , $k_{\text{cq}} = 8.0 \times 10^9 \text{ M}^{-1}\text{s}^{-1}$; Pt(bpy) Ph_2 , $k_{\text{cq}} = 3.7 \times 10^9 \text{ M}^{-1}\text{s}^{-1}$). However, the slowest cross-quenching rate ($k_{\text{cq}} = 0.2 \times 10^9 \text{ M}^{-1}\text{s}^{-1}$) was observed for Pt(bpy)(Mes)Cl in which a mesityl group is directly bound to the platinum center. From the crystal structures and electrochemistry of related complexes, it is anticipated that the mesityl ligand inhibits close approach of two platinum centers.²²



Though charge-transfer can be expected to play an important role in exciplex formation, the accumulated cross-quenching rates can be readily understood in terms of the steric properties of the quencher inhibiting close approach of the Pt(tmphen)(tdt) chromophore. For example, for the series of platinum bipyridyl quenchers shown in Figure 5, the cross-quenching rate decreases as the steric bulk of the substituents on the diimine increases. The least sterically-hindered quencher, Pt(bpy) Cl_2 , was found to be the most efficient quencher ($k_{\text{cq}} = 8.0 \times 10^9 \text{ M}^{-1}\text{s}^{-1}$), whereas the di-*t*-butyl substituted derivative, Pt(dbppy) Cl_2 , is the least efficient quencher ($k_{\text{cq}} = 2.3 \times 10^9 \text{ M}^{-1}\text{s}^{-1}$).

Steric effects also account for variations in quenching rates for a series of diphenyl platinum complexes with substituted phenanthroline ligands. Substitution of methyl groups at positions 3 through 8 of the phenanthroline ligand has negligible effect on the rate (e.g., Pt(phen) Ph_2 , $k_{\text{cq}} = 4.3 \times 10^9 \text{ M}^{-1}\text{s}^{-1}$; Pt(4,7-dmphen) Ph_2 , $k_{\text{cq}} = 4.3 \times 10^9 \text{ M}^{-1}\text{s}^{-1}$; Pt(3,4,7,8-tmphen) Ph_2 , $k_{\text{cq}} = 4.2 \times 10^9 \text{ M}^{-1}\text{s}^{-1}$). In contrast, methylation at the 2 and 9 positions of phenanthroline causes a significant decrease in the rate of quenching. In fact, the observed rate of quenching for Pt(2,9-dmphen) Ph_2 ($k_{\text{cq}} = 2.3 \times 10^9 \text{ M}^{-1}\text{s}^{-1}$) is slower than that of Pt(dpphen) Ph_2 ($k_{\text{cq}} = 2.6 \times 10^9 \text{ M}^{-1}\text{s}^{-1}$). The crystal structure of Pt(2,9-dmphen) Ph_2 shows that steric demands of the methyl groups result in large distortions relative to the geometry of Pt(phen) Ph_2 . The dihedral angle formed by the best fit plane for the diimine N=C-C=N atoms and the plane defined by the Pt center and two bonded carbon atoms is 31° .²¹ This distortion is anticipated to inhibit intermolecular diimine-diimine interactions, as well as Pt-Pt interactions. In addition, the methyl groups can be expected to protect the platinum center and restrict rotation of the phenyl ligands, further inhibiting close approach of two platinum complexes.



It is noteworthy that exciplex emission has not been observed for any cross-quenchers.⁷ This is not entirely surprising since excimer emission has not been observed in fluid solution for any platinum(II) diimine dithiolate complexes. It also is intriguing that the rate of quenching appears to be independent of the orbital character of the lowest excited-state of the platinum diimine quencher. For example, both Pt(dbbpy)Cl₂ ($k_{\text{cq}}=2.3 \times 10^9 \text{ M}^{-1}\text{s}^{-1}$) and Pt(dbbpy)(CN)₂ ($k_{\text{cq}}=2.1 \times 10^9 \text{ M}^{-1}\text{s}^{-1}$) quench the emission from Pt(tmphen)(tdt) at comparable rates, despite the fact that Pt(dbbpy)Cl₂ has a lowest ligand field excited state and Pt(dbbpy)(CN)₂ has a lowest $\pi-\pi^*$ excited state. The fact that these cross-quenching rates are similar to self-quenching rates is suggestive of a similar mechanism of quenching. The complex formed by association of a ground-state and excited-state molecule evidently has a non-emissive or weakly emissive lowest excited state that lies at lower energy than the MMLLCT state of Pt(tmphen)(tdt). The orbital character of this excited state is not certain, but the necessity of both platinum and a diimine ligand for rapid quenching suggests that orbitals centered on these groups are involved.

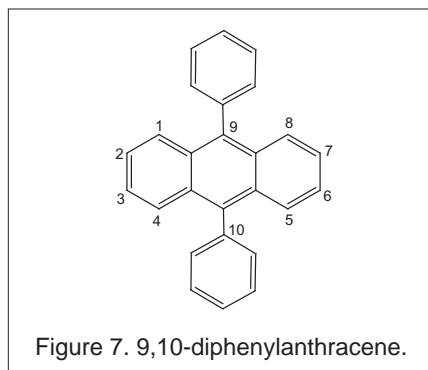


Figure 7. 9,10-diphenylanthracene.

The observed steric dependence of the cross-quenching rates is modest compared to other examples of quenching via exciplex formation. Emission from anthracene is quenched by dimethylaniline in cyclohexane through a charge-transfer interaction. Increasing phenyl substitution on the anthracene decreases the quenching rate by three orders of magnitude.²³ The rate is dependent upon the degree and position of substitution. For example, a greater decrease is reported for 1,4,5,8-tetraphenylanthracene ($k_{\text{q}}=0.02 \times 10^8 \text{ M}^{-1}\text{s}^{-1}$) than for 1,4-diphenylanthracene ($k_{\text{q}}=8.5 \times 10^8 \text{ M}^{-1}\text{s}^{-1}$). The fact that the rate is much slower for the 9,10-disubstituted anthracene ($k_{\text{q}}=0.5 \times 10^8 \text{ M}^{-1}\text{s}^{-1}$) than for the 1,4-disubstituted anthracene is consistent with the notion that the central ring is involved in the charge-transfer interaction (Figure 7). Similar changes in rate are observed for quenching of the emission from Cu(2,9-dmphen)₂⁺ by substituted pyridines binding to a vacant coordination site of the copper center. For example, the quenching rate for 2,6-dimethylpyridine ($k_{\text{q}} < 10^6 \text{ M}^{-1}\text{s}^{-1}$) of the copper complex is more than three orders of magnitude slower than that of pyridine ($k_{\text{q}}=10^9 \text{ M}^{-1}\text{s}^{-1}$).^{24,25} The weaker steric dependence of the cross-quenching rates may indicate longer intermolecular interactions for the platinum diimine systems. Indeed, the changes in rate with increasing steric bulk near the metal center are more dramatic than the changes associated with increasing steric bulk of the diimine ligand, as might be expected for a metal-metal interaction.

References

1. Chan, C. W.; Lai, T. F.; Che, C. M.; Peng, S. M. *J. Am. Chem. Soc.* **1993**, *115*, 11245-11253.
2. Drew, S. M.; Janzen, D. E.; Buss, C. E.; Macewan, D. I.; Dublin, K. M.; Mann, K. R. *J. Am. Chem. Soc.* **2001**, *123*, 8414-8415.
3. Miskowski, V. M.; Houlding, V. H. *Inorg. Chem.* **1989**, *28*, 1529-1533.
4. Cummings, S. D.; Eisenberg, R. *J. Am. Chem. Soc.* **1996**, *118*, 1949-1960.
5. Connick, W. B.; Miskowski, V. M.; Houlding, V. H.; Gray, H. B. *Inorg. Chem.* **2000**, *39*, 2585-2592.
6. Hissler, M.; Connick, W. B.; Geiger, D. K.; McGarrah, J. E.; Lipa, D.; Lachicotte, R. J.; Eisenberg, R. *Inorg. Chem.* **2000**, *39*, 447-457.
7. Fleeman, W. L.; Connick, W. B. *Comments on Inorganic Chemistry* **2002**, *23*, 205-230.
8. Che, C.-M.; Wan, K.-T.; He, L.-Y.; Poon, C.-K.; Yam, V. W.-W. *J. Chem. Soc., Chem. Commun.* **1989**, 943-945.
9. Kunkely, H.; Vogler, A. *J. Am. Chem. Soc.* **1990**, *112*, 5625-5627.
10. Chan, C.-W.; Che, C.-M.; Cheng, M.-C.; Wang, Y. *Inorg. Chem.* **1992**, *31*, 4874-4878.
11. Connick, W. B.; Marsh, R. E.; Schaefer, W. P.; Gray, H. B. *Inorg. Chem.* **1997**, *36*, 913-922.
12. Pettijohn, C. N.; Jochowitz, E. B.; Chuong, B.; Nagle, J. K.; Vogler, A. *Coord. Chem. Rev.* **1998**, *171*, 85-92.
13. Wan, K.-T.; Che, C.-M.; Cho, K.-C. *J. Chem. Soc., Dalton Trans.* **1991**, 1077-1080.
14. Connick, W. B.; Geiger, D.; Eisenberg, R. *Inorg. Chem.* **1999**, *38*, 3264-3265.
15. Connick, W. B.; Gray, H. B. *J. Am. Chem. Soc.* **1997**, *119*, 11620-11627.
16. Kato, M.; Sasano, K.; Kosuge, C.; Yamazaki, M.; Yano, S.; Kimura, M. *Inorg. Chem.* **1996**, *35*, 116-123.
17. Buchner, R.; Cunningham, C. T.; Field, J. S.; Haines, R. J.; McMillin, D. R.; Summerton, G. C. *J. Chem. Soc., Dalton Trans.* **1999**, *5*, 711-717.

18. Kato, M.; Kosuge, C.; Morii, K.; Ahn, J. S.; Kitagawa, H.; Mitani, T.; Matsushita, M.; Kato, T.; Yano, S.; Kimura, M. *Inorg. Chem.* **1999**, *38*, 1638-1641.
19. Kato, M.; Kozakai, M.; Fukagawa, C.; Funayama, T.; Yamauchi, S. *Mol. Cryst. Liq. Cryst.* **2000**, *343*, 353-358.
20. Demas, J. N. *Static or Associational Quenching*; Academic Press: New York, 1983; pp 52-65.
21. Klein, A.; McInnes, E. J. L.; Kaim, W. J. *Chem. Soc., Dalton Trans.* **2002**, 2371-2378.
22. Klein, A.; Kaim, W. *Organometallics* **1995**, *14*, 1176-1186.
23. Lishan, D. W.; Hammond, G. S.; Yee, W. A. J. *Phys. Chem.* **1981**, *85*, 3435-3440.
24. McMillin, D. R.; Kirchoff, J. R.; Goodwin, K. V. *Coord. Chem. Rev.* **1985**, *64*, 83-92.
25. Horvath, A.; Stevenson, K. L. *Coord. Chem. Reviews* **1996**, *153*, 57-82.

About the Authors

Wendi Fleeman received her B.A. from Transylvania University in 1998 and is currently a graduate student at the University of Cincinnati. While at the University of Cincinnati her research has focused on understanding the photophysical properties of platinum(II) diimine complexes. She has received grant support from the University of Cincinnati Department of Chemistry Research Associates Program (1998-2001) and the University of Cincinnati Research Council (2000-2001). She was also awarded the Twitchell-Stecker fellowship from the Department of Chemistry (2001-2002).

Bill Connick is an Assistant Professor of Chemistry at the University of Cincinnati. After earning his undergraduate degree from Williams College in 1988, he studied for two years at the University of Cambridge where he obtained a M.A. degree in chemistry. In 1997, he obtained his Ph.D. from the California Institute of Technology while working with Professor Harry Gray. After completing a postdoctoral appointment in the laboratory of Professor Rich Eisenberg at the University of Rochester, he joined the faculty at the University of Cincinnati in 1998. He has received a Beckman Young Investigator Award from the Arnold and Mabel Beckman Foundation and a National Science Foundation CAREER Award for his research focused on engineering metal complexes for photoinduced two-electron transfer.

Copyright 2002 by the Center for Photochemical Sciences
The Spectrum is a quarterly publication of the Center for
 Photochemical Sciences, Bowling Green State University,
 Bowling Green, OH 43403.
 Phone 419-372-2033 Fax 419-372-0366
 Email photochemical@listproc.bgsu.edu
 WWW <http://www.bgsu.edu/departments/photochem/>

Executive Director:	D. C. Neckers
Principal Faculty:	P. Anzenbacher, G. S. Bullerjahn, J. R. Cable, F. N. Castellano, M. E. Geusz, D. C. Neckers, M. Y. Ogawa, V. V. Popik, M. A. J. Rodgers, D. L. Snavely, B. R. Ullrich
<i>The Spectrum</i> Editor:	Pat Green
Production Editor:	Alita Frater

COPYRIGHT PERMISSION

A person may make a single copy of any or all articles in this issue for personal use. Copying beyond that permitted by the U.S. Copyright law is allowed provided that the appropriate per copy fee is paid through the Copyright Clearance Center, Inc., 27 Congress St., Salem, MA 01970. For reprint permission, please write to the Center for Photochemical Sciences.

EDITORIAL POLICY

The Spectrum reserves the right to review and edit all submissions. The Spectrum is not responsible for contents of articles.

Articles submitted to The Spectrum will appear at the discretion of the editorial staff as space is available.

Science and Technology of Organic Light Emitting Diodes

from basic chemistry and physics to high resolution organic displays

Willi Graupner
austriamicrosystems AG, Austria

Introduction

Light emitting diodes (LEDs) generate light from optical transitions following the recombination of electrons and holes in the active, emitting layer of the device. LEDs, in general, were viewed as the light source of the future due to their longevity, compactness, efficiency and many other advantages. For this reason there have been tremendous research and development activities, which boosted the achievable light output at constant electrical input by a factor of 10 over the last decade. At the same time we have seen LEDs used in many daylight display applications, the one in traffic lights perhaps is the most obvious one.

Organic LEDs (OLEDs), that is, devices where the semiconducting charge transport and light emitting layers are made from organic molecules, have attracted tremendous attention recently because it is anticipated that their production is easy and hence inexpensive. The thermal budget of inorganic device production processes and cost is much higher for inorganic devices than for organic ones. The potential of simple ink jet printing of organic electronics has even further nurtured the cost-related hopes. In addition, the ease of controlling electronic transport and emission properties (= color - see ref. 1) via simply choosing different molecules allows for a tremendous variety of device properties which can easily be optimized by choosing or building the right molecule.¹

In particular, OLEDs can be built in a planar fashion, very suitable for display purposes. With the flat panel display business being a several 10 billion dollar market worldwide, the OLED R&D efforts are very worthwhile if a fraction of this market can be conquered.

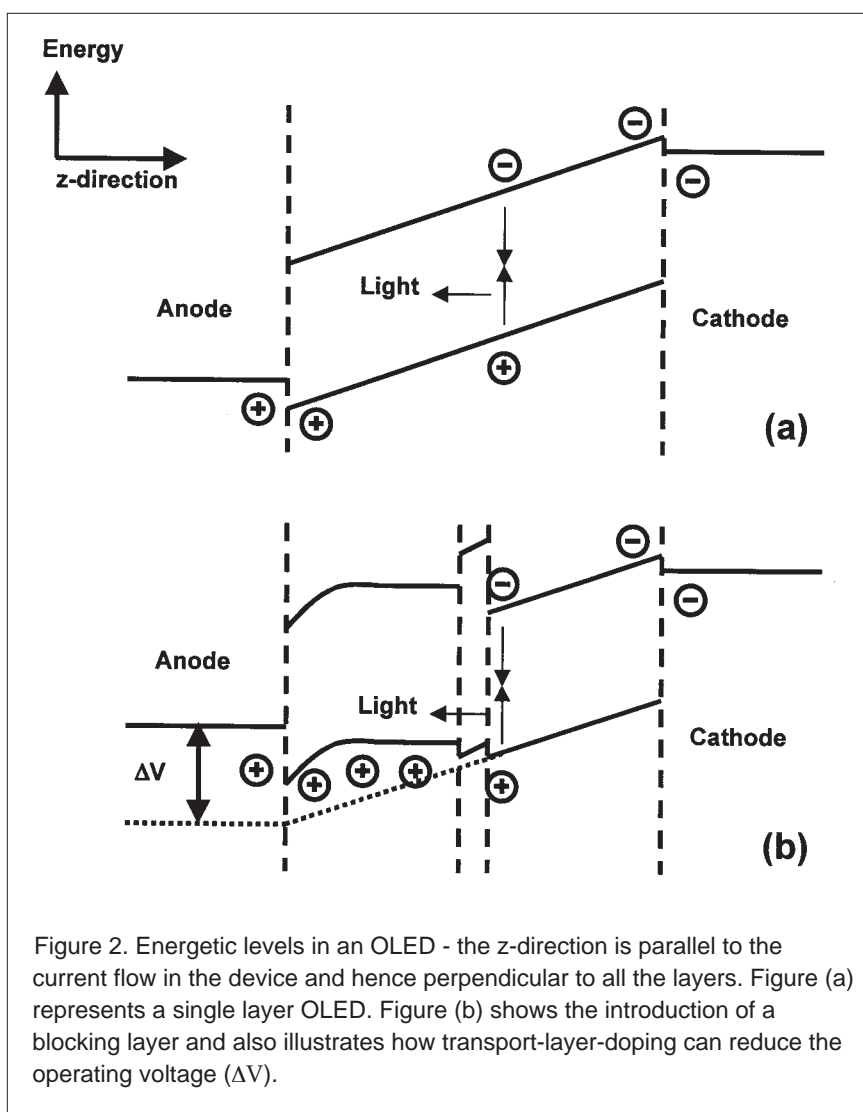
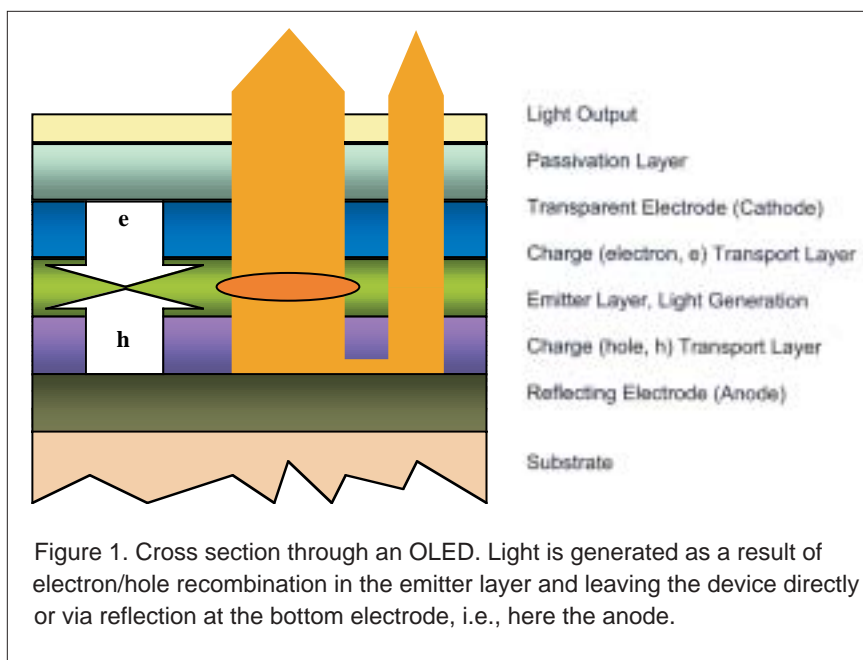
Device Physics

In order to understand the importance of chemistry for OLEDs, one only needs to look at the basic rules of operation of an **ideal light emitting diode**. In parentheses the commonly used technical terms are mentioned:

1. Equivalent amounts of electrons and holes (current balancing)
2. shall be injected into the active layer (injection efficiency)
3. and transported within the active layer (mobility)
4. at sufficiently low voltages which barely change during operation (stability)
5. in order to recombine completely in the emitter zone (recombination probability)
6. and yield radiative transitions exclusively (radiative efficiency)
7. which create photons of the right color (emission spectrum)
8. with the photons being able to leave the LED without scattering, absorption and reflection losses (output coupling efficiency)

Of course this ideal LED does not exist (yet). But, this "simple guideline" determines the work of device and circuit designers, material scientists as well as chemists and process engineers. One of the most basic conclusions from the previous list is that OLEDs have to be multi-component devices with different components having different functionalities. All components need to be stable, but only one electrode needs to be highly transmissive. Only the emitter layer should show a high recombination probability; the charge transport layers need high mobility, and so forth (ref. 1).

Figure 1 describes the most commonly used approach to build OLEDs. The organic stack is sandwiched between a reflecting and nearly transparent metal electrode for optimum light output. The green arrows illustrate the reflection of a fraction of light at the bottom electrode. Electrode design has to be a compromise between the bulk properties (i) conductivity and (ii) absorption and the interface properties (iii) work function, (iv) adhesion to the organic layer and (v) reflectivity. The shaded structures in Figure 1 express the resulting multi-component-nature of the electrodes: alloys, multi layer, graded composition layer, and so forth. This paper will not focus on these inorganic/metallic parts



of the OLEDs. Even the three different organic layers are often multi-component in nature. Their composition again reflects a compromise between interface and bulk properties.

It will be the focus of this paper to describe research and development efforts, mainly in chemistry, but also physics and engineering to approach the ideal OLED as closely as possible. The arguments given in this paper are correct but often highly simplified. Therefore, I highly recommend reference 2 for a detailed and deep understanding of OLED device physics.

Injection of Charge Carriers

The injection of charges from a metal layer into a bulk organic film is determined by many parameters, the most crucial being the matching of energy levels. The metal work function has to match the highest occupied molecular orbital (HOMO) for hole injection and the lowest unoccupied molecular orbital (LUMO) of its organic counterpart for electron injection.³ This principle is illustrated in Figure 2 (a). The practical implication is that a proper materials combination has to be found both for the cathode/electron-transport-layer and anode/hole-transport-layer interface, respectively. The choice of different electrode materials for the same organic charge transport layer can change the energy level mismatch between the layers by a few tenths of electron volts which corresponds to variations of the charge injection efficiency, and hence injected currents, of several orders of magnitude.³ A quick overview of commercially available organic transport materials can be obtained from reference 1.

However, energy levels should always be seen in context with other properties: melting point, glass transition temperature, oxidation potential, absorption and emission wavelengths of hole transport materials that can be varied very systematically as shown in reference 4. In this particular example different amines are bound to positions 1 and 4 of a benzene

molecule. Indeed, this work lies at the heart of many OLED hopes: a combined variation/optimization of mechanical, electrical and optical properties of layers by the sole application of organic synthesis. Having such customizable building blocks at hand allows for the full application of OLED design principles. The combination of several properties is absolutely critical. Two polymers with **similar emission colors**, that is, similar HOMO-LUMO difference, but very different absolute HOMO and LUMO values need **different electrode materials** to optimize charge injection efficiency.⁵ A wrong combination of materials at this interface can decrease injection efficiency by several orders of magnitude!⁵

Aside from choosing the right **combination** of materials, it is also important to look for some properties of the charge transport material alone. Further improvement can be gained by using high mobility transport materials. Injection efficiency can be increased by a mobility increase of the transport material.⁶ Finally, the electronic bandwidth of the charge transport layer needs to be mentioned. In brief, the broader the bandwidth, the higher the injection efficiency.⁷

Charge Transport

In the previous section it became clear how mobility, bandwidth and HOMO/LUMO levels of the transport materials influence injection efficiency. In contrast, this section is dedicated to their charge transport as well as charge blocking properties. The primary requirement for an electron/hole transport material is to exhibit high electron/hole mobility. Increasing mobility decreases the voltage drop across the transport layer at constant current. Hence, the quest for better/new materials and film processing is driven by the achievable mobility values. However, charge transport layers also have another vital function. They can act as “counter-charge” blocking layers.

Figure 2 (b) shows the advantageous effect of a hole transport structure which does not allow electrons to leave the emitter region thereby forcing recombination to occur in the emitter region. In this particular case the hole transport layer has also been doped for various reasons. The application of transport layer doping increases conductivity and enables decreasing the depletion region near the anode (note how the transport layer energetics vary between Figures (a) and (b)). In order to achieve electron blocking, a thin blocking layer is inserted between the hole transport layer and the emitter. In both Figures (a) and (b) the emitter layer also functions as the electron transport layer. For this particular device⁸ the brightness of a PC-monitor of about 100 cd/m² is reached at an operating voltage of 3.2 V—the lowering of the operating voltage can be seen from a comparison of Figures 2 (a) and (b) since the energetics of the emitter layer (i.e., color) are the same in both devices. A current density of 100 mA/cm² is reached at 4.5 V, leading to an overall light/current efficiency of 5 cd/A.⁸

High Radiative Recombination Efficiency

The previous section has already shown one way to increase recombination efficiency by device design: confinement of the carriers in the emitter region via charge blocking. There are several more issues to address.

First, it is known that different molecules show different probabilities for radiative recombination. Second, it has been shown that doping a host layer with a proper emitter guest, typically at the one percent level, leads to a much more efficient emitter emission, that is, a higher radiative recombination probability, than in the emitter-only layer.⁹ This approach also allows to tune the color. Based on an appropriate combination of guest and host emission white OLEDs can be built.¹⁰ Third, and finally, it is known only very recently¹¹ that the formation of emissive singlet states versus non-emissive triplet states is material dependent—a property which was believed to be identical for all emitters. Summarizing these three arguments, choosing the proper molecules—and combination in the case of doping—is essential. We should also not forget that many of these molecules were only developed over the last years because of the OLED-driven research.

Stability

The typical long-term test condition for an OLED is to monitor driving voltage and brightness at constant current. While we would like to see no change over time, we typically observe an increase of voltage and a decrease of brightness—the former creating a problem for the driver circuitry, the latter for the user.

For commercial display and lighting applications a very general requirement of stability can be phrased like this: the device should not decrease its brightness by more than 50% within the first 10,000 hours. The precise conditions will strongly depend on the application. In a display, for example, the differential aging of neighboring pixels or pixels with different colors is much more annoying than an overall loss of brightness, since differential aging of pixels will result in remnant images and change of the color balancing. Screen savers are one way to avoid differential aging.

It is essential to understand the underlying degradation mechanisms of OLEDs in order to define the proper counter strategies. Commercially available OLED displays by Pioneer show that proper packaging via glass sealing combined with substantial amounts of getter material can prevent air and moisture from attacking the organic layers. Other companies have pursued different paths.¹²

However there is more to the story than environmental influence. It has been shown by various authors that running OLEDs as electron-only or hole-only devices under inert conditions can result in extremely different stability behavior¹³. For example, while electron-only devices showed a voltage increase of 30 mV/hour when driven at 8.3 mA/cm² and at 85 °C, hole-only devices showed changes smaller than 1 mV/hour under the same conditions. The difference of 1 and 30 mV/hour means a factor 30 in device degradation behavior for electron and hole only devices made from the same material. Hence, we have to conclude that the presence of electrons or holes in certain organic layers triggers instability. Their absence on the other hand seems to enable stability. There is no surprise in this fact: it is a simple consequence of molecules showing different susceptibility to oxidative or reductive attack. Therefore, one needs to perform these single-carrier studies for the devices and materials of choice.

In general, device degradation of OLEDs can be the consequence of (1) chemical reactions of the active materials, triggered by electrons, holes, light, water, oxygen and combinations thereof as well as (2) structural changes in the layers/interfaces triggered by temperature or chemical reactions. While packaging optimization and single-carrier tests address the chemical issue, molecular films are also being screened for their temperature behavior—systematic material development can also help there.⁴

Small Molecules Versus Polymers

One of the most interesting questions in the OLED field is whether small molecules or polymers will make the race—or whether they will even coexist in different applications. While there is no big difference in the fundamental device functionalities, processing, electronic and structural properties can be very different and make the choice a technology-enabling or preventing question and have strong implications on device costs. In summary, it should be mentioned that small-molecule based OLEDs by Pioneer have been on the market for several years while polymeric ones have appeared this summer (2002). Based on small molecules, it was easier to reach all the requirements for an industrial production process, in particular, reproducibility. The big disadvantage of small-molecule-based OLEDs is cost. So far they have been produced by expensive physical vapor deposition of the molecules. Polymeric layers can be applied much more cost effectively via spin coating, roll-to-roll processes and other techniques. Ink jet printing might be available for both material classes and enable us even to produce application specific displays (ASD) cost effectively. Polymeric layers withstand thermal and mechanical stress much better than small-molecule based layers. The big advantage of small molecules over polymers so far lies in the better defined and reproducible synthesis and purification procedures as well as in higher charge carrier mobilities. With the latter problems being solved now, cost will most likely drive industry away from using physical vapor deposition techniques.

Summary and Outlook

About 15 years after the groundbreaking scientific reports on small molecule¹⁴ and polymeric¹⁵ OLEDs, the science and engineering leaders in the field can now identify topics for the OLED technology roadmap. Issues such as phosphorescent small molecules, spin-dependent exciton formation, white-emitting OLEDs, lighting applications, coating technologies, flexible substrates, device reliability and light output coupling will need major further development. These topics all boil down to two key problems for a broad market penetration by OLEDs in several brightness and resolution ranges:

- to have the right molecules at high levels of purity available in order to fully exploit and apply our quite clear understanding of the device physics
- to find a stable cost-effective industrial production process.

This means there is still a lot of exciting materials science and chemistry ahead as well as highly interdisciplinary work with manufacturing engineers.

References

1. H. W. Sands Corp. e.g. lists OLED materials by function http://www.hwsands.com/productlists/oled/cross_reference_material_function_oled.htm and also provides a good overview of emitter molecules of different color http://www.hwsands.com/productlists/oled/oled_emitters_color_emission.htm.

2. Ruhstaller, B.; Carter, S. A.; Barth, S.; Riel, H.; Riess, W.; Scott, J. C. *J. Appl. Phys.* **2001**, *89*, 4575-4586.
3. Abkowitz, M.; Facci, J. S.; Rehm, J. *J. Appl. Phys.* **1998**, *83*, 2670-2676.
4. Koene, B. E.; Loy, D. E.; Thompson, M. E. *Chem. Mater.* **1998**, *10*, 2235-2250.
5. Campbell, A. J.; Bradley, D. D. C.; Antoniadis, H. *J. Appl. Phys.* **2001**, *89*, 3343-3351.
6. Shen, Y.; Klein, M. W.; Jacobs, D. B.; Scott, J. C.; Malliaras, G. G. *Phys. Rev. Lett.* **2001**, *86*, 3867-3870.
7. Kalinowski, J. *J. Phys. D: Appl. Phys.* **1999**, *32*, R179-249.
8. Zhou, X.; Pfeiffer, M.; Blochwitz, J.; Werner, A.; Nollau, A.; Fritz, T.; Leo, K. *Appl. Phys. Lett.* **2001**, *78*, 410-412.
9. Tasch, S.; List, E. J. W.; Hochfilzer, C.; Leising, G.; Schlichting, P.; Rohr, U.; Geerts, Y.; Scherf, U.; Müllen, K. *Phys. Rev. B* **1997**, *56*, 4479-4483.
10. Tasch, S.; List, E. J. W.; Ekstrom, O.; Graupner, W.; Leising, G.; Schlichting, P.; Rohr, U.; Geerts, Y.; Scherf, U.; Müllen, K. *Appl. Phys. Lett.* **1997**, *71*, 2883-2885.
11. Wohlgenannt, M.; Tandon, K.; Mazumdar, S.; Ramasesha, S.; Vardeny, Z. V. *Nature* **2001**, *409*, 494-496; Wilson, J. S.; Dhoot, A. S.; Seeley, A. J. A. B.; Khan, M. S.; Kohler, A.; Friend, R. H. *Nature* **2001**, *413*, 828-831.
12. Graupner, W.; Heller, C. M.; Ghosh, A. P.; Howard, W. E. *SPIE Proceedings* **2000**, *4207*, 11-19.
13. Parker, I. D.; Cao, Y.; Yang, C. Y. *J. Appl. Phys.* **1999**, *85*, 2441-2447.
14. Tang, C. W.; VanSlyke, S. A. *Appl. Phys. Lett.* **1987**, *51*, 913-915.
15. Burroughes, J. H.; Bradley, D. D. C.; Brown, A. R.; Marks, R. N.; Mackay, K.; Friend, R. H.; Burns, P. L.; Holmes, A. B. *Nature* **1990**, *347*, 539-541.

About the Author

Willi Graupner received his Ph.D. at the Technical University of Graz in 1994, where he studied optical and structural properties of conjugated molecules. He completed his Habilitation in Experimental Condensed Matter Physics in Graz 1998 moved on as an Assistant Professor for Physics and Materials Science and Engineering at Virginia Tech. After a one-year engagement at www.eMagin.com, working in the field of active matrix OLEDs, he is now heading the process integration group at www.austriamicrosystems.com. He can be reached at ++43 3136 500 4147 or willi.graupner@austriamicrosystems.com.

Center Ph.D. Student Recognized for Excellence

Bilal Kaafarani, a fourth year doctoral student in photochemical sciences at Bowling Green State University, received several very distinguished awards from the University.

Bilal, a student of McMaster Distinguished Professor D. C. Neckers, was named Outstanding International Student and was a finalist for a Research Assistant Award. In addition, he received the top honor accorded a graduate student, the Charles Shanklin Award, in recognition of excellence in original research by graduate students at Bowling Green State University.

Bilal is from Lebanon and is one of 550 international graduate students attending BGSU.